A strong-motion database from the Central American subduction zone

Maria Cristina Arango, Fleur O. Strasser, Julian J. Bommer, Douglas A. Hernández, Jose M. Cepeda

A STRONG-MOTION DATABASE FROM THE CENTRAL AMERICAN SUBDUCTION ZONE

M.C. Arango [1], F.O. Strasser[2], J.J. Bommer[1*], D. Hernández[3], & J.M. Cepeda[4]

1. *Department of Civil & Environmental Engineering, Imperial College London, London SW7 2AZ, UK*
2. *Seismology Unit, Council for Geoscience, Private Bag X112, Pretoria 0001, South Africa*
3. *Departamento de Sismologia, SNET, San Salvador, El Salvador*
4. *International Centre for Geohazards, NGI, Oslo, Norway*

ABSTRACT

Subduction earthquakes along the Pacific Coast of Central America generate considerable seismic risk in the region. The quantification of the hazard due to these events requires the development of appropriate ground-motion prediction equations, for which purpose a database of recordings from subduction events in the region is indispensable. This paper describes the compilation of a comprehensive database of strong ground-motion recordings obtained during subduction-zone events in Central America, focusing on the region from 8 to 14ºN and 83 to 92ºW, including Guatemala, El Salvador, Nicaragua and Costa Rica. More than 400 accelerograms recorded by the networks operators across Central America during the last decades have been added to data collected by NORSAR in two regional projects for the reduction of natural disasters. The final database consists of 554 triaxial ground-motion recordings from events of moment magnitudes between 5.0 and 7.7, including 22 interface and 58 intraslab-type events for the time period 1976-2006. Although the database presented in this study is not sufficiently complete in terms of magnitude-distance distribution to serve as a basis for the derivation of predictive equations for interface and intraslab events in Central America, it considerably expands the Central American subduction data compiled in previous studies and used in early ground-motion modelling studies for subduction events in this region. Additionally, the compiled database will allow the assessment of the existing predictive models for subduction-type events in terms of their applicability for the Central American region, which is essential for an adequate estimation of the hazard due to subduction earthquakes in this region.

Keywords: Central American subduction zone, strong-motion database, ground-motion processing, site classes, seismological parameters.

* Corresponding author: T: +44-20-7594-5984, F: +44-20-7594-5934, E: j.bommer@imperial.ac.uk

1. INTRODUCTION

This paper discusses the compilation of a comprehensive database of ground motions from subduction-zone earthquakes in Central America for the period 1976-2006, focusing on the region from 8ºN to 14ºN and 83ºW to 92ºW, including Guatemala, El Salvador, Nicaragua and Costa Rica. A similar study is presented in a companion paper (Arango *et al.*, 2010) for ground motions from the Peru-Chile subduction zone. The seismicity of Central America is the result of the interaction of five tectonic plates, namely the North American, Caribbean, Cocos, Nazca and South American plates (Figure 1). The Cocos plate borders the Caribbean and North American plates by the Central American subduction zone along the Middle American Trench. To the north, the North American plate borders the Caribbean plate along a left-lateral transform boundary which, in Central America, is marked by the Motagua-Polochic fault system. In the west, the East Pacific Rise forms the border between the Pacific plate and the Cocos plate. To the South, the Nazca plate borders the Cocos plate along the Galapagos rift.

The distribution of seismicity along the Central American subduction zone is shown in Figure 1, in addition to a number of cross-sections of seismicity taken along the strike of the trench. The hypocentre locations have been obtained from the Engdahl-Hilst-Buland (EHB) Bulletin for the period 1960-2006 (Engdahl *et al.*, 1998) available at http://www.isc.ac.uk/EHB/index.html). The dominating part of the seismicity in the region is associated with the subduction of the Cocos plate beneath the Caribbean and North American plates. Convergence rates for the Cocos plate under the North American and Caribbean plates range from ~50 mm/year along the coast of Mexico to ~95 mm/year off southern Costa Rica (DeMets, 2001). The age of the subducted Cocos plate also varies along the strike of the trench from ~20-30 Ma under Nicaragua and northern Costa Rica to ~20-22 Ma and 13-17 Ma beneath central and southern Costa Rica respectively. Cross-sections of seismicity along the main axis of Central America (Figure 1) show shallow-focus seismicity, which is associated with volcanism and forearc deformation of the Caribbean plate. A 1200 km-long volcanic arc extends from the Mexico-Guatemala border to central Costa Rica, but Quaternary volcanism is absent in southern Costa Rica. Other regions with important seismic activity include the Motagua-Polochic fault system, the North Panama Deformed Belt and the Panama fracture zone.

In the region of interest, earthquakes associated with the subduction of the Cocos plate beneath the Caribbean plate are of two types: events occurring along the contact between the Cocos and Caribbean plates (interface earthquakes) and events associated with the internal deformation of the Cocos plate (intraslab earthquakes). Interface events in this region have focal mechanisms consistent with their occurrence as reverse motion on shallow-dipping planes, whereas intraslab earthquakes typically have focal mechanisms consistent with their occurrence as normal faulting caused by extension. Several authors (*e.g.*, LeFevre & McNally, 1985; Bilek & Lay, 1999; Protti *et al.*, 1994;) have discussed aspects of the Central America subduction zone such as the geometry of the subducted Cocos slab, the regional distribution of stresses and characteristics of the plate interface.

Large (M=7.0) subduction-zone earthquakes regularly cause widespread damage throughout the Central American region. Although generally less destructive than crustal events, whose shallower depths and proximity to densely populated areas can lead to substantial damage and heavy social losses even for moderate-magnitude events such as the 23 December 1972 Managua and 10 October 1986 San Salvador events, large subduction-zone events can nevertheless result in heavy losses, occasionally due to the triggering of tsunamis. A clear example of this was 2 September 1992 (M_S 7.2, M_W 7.6) earthquake, which occurred as thrust faulting on the Cocos-Caribbean plate interface off the coast of Nicaragua (Satake, 1995; Kanamori & Kikuchi, 1993), causing important damage: at least 116 people were killed and 1300 houses were destroyed. Most of the damage and causalities of this event were caused by a tsunami that affected the west coast of Nicaragua and Costa Rica, reaching heights of up to 8 m (Ambraseys & Adams, 2001). In general, damage due to subduction earthquakes in Central America however is the result of shaking of long duration, which tends to cause extensive damage to vulnerable local building types such as *adobe* and also has been seen to have a high potential to trigger landslides (Bommer & Rodríguez, 2002). For example, the 13 January 2001 M_w 7.7 intraslab event, the largest earthquake to occur in Central America in recent years, claimed almost 1200 lives, causing widespread damage and triggering numerous landslides (Bommer *et al.*, 2002).

Large earthquakes have also occurred off the Pacific coast of Costa Rica due to subduction processes. A large (M_S 7.7) underthrusting event occurred on 5 October 1950 offshore the Nicoya Peninsula. This segment has been identified as a seismic gap, where a large earthquake is expected to occur in the near future (Nishenko 1989; Protti *et al.*, 2001). More recently, a relatively large magnitude event occurred on 25 March 1990 (M_W 7.3) event at the entrance of the Nicoya Peninsula. Although this latter event was initially associated with a rupture along the Nicoya seismic gap, detailed studies (Protti *et al.*, 1995; Husen *et al.*, 2002) indicated that the event was located to the southeast of the gap and instead it was due to the rupture of a seamount which acted as an asperity.

Since subduction-zone earthquakes are one of the main sources contributing to the seismic hazard in Central America, the derivation of ground-motion predictive models for both interface and intraslab events that are applicable to the Central American region is essential step towards better estimation of earthquake hazard in this region. The development of robust predictive models for interface and intraslab-type earthquakes in Central America has been, however, hampered by the limited availability of a database of subduction-zone ground motions and associated seismological parameters. This has led to seismic hazard studies for Central America adopting global (Youngs *et al.*, 1997) and Japanese (Zhao *et al.*, 2006) ground-motion models for subduction-zone earthquakes (Benito Oterino *et al.*, 2009). These two models were selected for the regional PSHA conducted by Benito Oterino *et al.* (2009), from among a selection of global and regional models, on the basis of inspection of residuals calculated for recorded motions from the region. The PGA residuals were calculated using 439 recordings from subduction events but for spectral accelerations at 0.3 and 1.0 seconds, the study made use of only 75 records. In the present study, we characterise more than 550 recordings from subduction-zone earthquakes in Central America.

A first effort to collect and digitise all strong-motion data recorded in Central America was made by NORSAR in the 1990's, with funding from the Research Council of Norway in two projects: "Reduction of Natural Disasters in Central America, Earthquake Preparedness and Hazard Mitigation - Establishment of Local and Regional Data Centres" and "Reduction of Natural Disasters in Central America - Earthquake Preparedness and Hazard Mitigation Phase II". The recordings collected during these projects and associated metadata have been re-processed and documented by Douglas *et al.* (2004). This earlier

database, hereafter referred to as the Douglas *et al.* (2004) database, contains 308 triaxial strong-motion accelerogram recordings from both shallow-crustal and subduction-zone earthquakes that have been recorded in Central America until 1996.

In this study, more than 400 additional accelerograms from subduction events recorded by the network operators across Central America during the last decades have been merged with subduction ground-motions included in the Douglas *et al.* (2004) database to create a single database of Central American subduction ground motions and associated metadata parameters for the period 1976-2006. The characteristics of the compiled database are summarised in Table 1 alongside details on data availability. The present paper describes the work performed in order to develop this database, with a particular emphasis on methodological aspects of metadata selection and ground-motion processing. A flat file with the compiled database is provided as an electronic supplement to this paper.

2. STRONG-MOTION NETWORKS IN CENTRAL AMERICA

The location of the stations contributing strong-motion recordings to this study is shown in Figure 2. The coordinates of the stations, type and location of the instruments are summarised in Tables 2 to 5, as obtained from the header information included by the network operators in the time-series files. In instances where complete station information was not included in the headers, the necessary data were retrieved from the website of the network operators directly. These station data were supplemented by information obtained from a number of studies including EERI (1991), Taylor *et al.* (1994), Bommer *et al.* (1997), Douglas *et al.* (2004), Cepeda *et al.* (2004), Climent *et al.* (2007), in particular to determine parameters for stations that are no longer in operation.

Strong-motion networks are currently operating in Guatemala, El Salvador, Costa Rica, Nicaragua and Panama. Only two Central American countries, Belize and Honduras, presently have no accelerometric networks in operation. In Guatemala, four accelerographs were installed as temporary stations following the 4 February 1976 (M_W 7.5) earthquake which affected Puerto Santo Tomás, Zacapa, Chichicastenango, and Guatemala City. These stations recorded some of the aftershocks associated with this event, prior to which only one accelerograph was operating at the Observatorio Nacional in Guatemala City. In 2001, a network of 12 digital accelerographs was deployed as part of a

project of the National Commission for Disaster Reduction (CONRED), eight of which were located within the urban limits of Guatemala City, and four towards the south-western side of the city. All these instruments are three-component Kinemetrics QDR model accelerographs.

In El Salvador, the first strong-motion instruments were deployed in 1960s by the Geotechnical Investigation Centre (CIG). By 1991, the CIG network consisted of more than 50 SMA-1 analogue accelerographs distributed around San Salvador and different cities around the country. The CIG network operated continuously until 1995 when it was restructured. The new configuration consisted of 26 accelerographs, 10 of which were installed as a three-dimensional array in San Salvador. Four more were installed at the Central American University (UCA), the Geotechnical Investigation Centre (CIG), the Seismological Observatory (OB) and Soyapango (SO) in San Salvador, with the remaining instruments distributed throughout El Salvador. Following the earthquake sequence that struck El Salvador in 2001, the local government created the National Service of Territorial Studies (SNET), which is the institution currently in charge of the seismic monitoring and operation of the strong-motion network. The SNET network, originally operated by CIG, was upgraded and restructured and presently consists of 13 ETNA digital accelerographs and 10 SMA-1 analogue instruments, which were upgraded to digital format. The network operated by UCA consists of 10 Kinemetrics SSA-2 digital accelerographs. The UCA network was designed to provide coverage of seismicity from both the subduction zone and the volcanic chain zone. A comprehensive description of this network is presented by Bommer *et al.* (1997). Finally, 14 more digital accelerographs are operated by the Hydroelectric Commission of the Lempa River (CEL) and the Salvadorean Geothermal Company (LAGEO) in El Salvador. These instruments are located at hydroelectric power plants in the Lempa River basin and at the Berlín geothermal field.

In 1975, the Seismic Research Institute of Nicaragua (IIS) installed an accelerographic network consisting of 47 instruments. A network of 16 telemetric stations was also installed that same year. These networks were in full operation until 1982, when their operation was gradually suspended due to the socioeconomic problems in Nicaragua at that time. The Nicaraguan Institute of Territorial Studies (INETER) was created in 1991, and placed in charge of re-establishing the telemetric seismic network and the existing accelerographic instruments. In 1997, seven K2 Kinemetrics accelerographs were temporarily installed in

Managua in order to gather information for the Seismic Microzonation of Managua project as part of the Seismic Hazard in Central America study financed by the Norwegian Agency for Development Cooperation (NORAD). In 1999, a new accelerograph network was deployed by the INETER in Managua and other major cities along the northern Pacific coast of Nicaragua. Presently, the INETER network consists of 17 ETNA digital instruments permanently operating in the principal cities of Nicaragua: Managua (five stations), Masaya, Granada, Jinotega, Matagalpa, Juigalpa, Boaco, Somoto, Ocotal, Estelí, Rivas, Chinandega and León.

In 1984 a strong-motion instrumentation programme started at the University of Costa Rica. A strong-motion network consisting of 20 accelerographs was deployed. In 1989, the Earthquake Engineering Laboratory (LIS) of the University of Costa Rica was established, having responsibility for the operation of the strong-motion network in Costa Rica. Presently, two institutions are mainly involved with the operation of strong-motion networks in Costa Rica: LIS and the Costa Rican Institute of Electricity (ICE). The LIS network originally consisted of 25 SMA-1 analogue instruments, which were gradually replaced by SSA and ETNA accelerographs. Currently, the LIS network consists of 33 stations located in the central region of Costa Rica and along the Pacific coast. The ICE operates 15 accelerographs installed at nine different sites: 4 of the stations are located in the free field and the rest are located on dams.

3. DATABASE DESCRIPTION

The starting point for the database compiled during this study was the data collected by NORSAR in two projects: "Reduction of Natural Disasters in Central America, Earthquake Preparedness and Hazard Mitigation - Establishment of Local and Regional Data Centres" and "Reduction of Natural Disasters in Central America - Earthquake Preparedness and Hazard Mitigation Phase II". The collected strong-motion data consisted of 308 records from shallow-crustal and subduction events from 1966 to 1996, which have been re-processed, documented and disseminated to the wider seismological and engineering community (Douglas *et al.,* 2004). Only records from subduction-zone ground motions have been taken from this early database and 400 more accelerogram recordings from subduction-zone events recorded by the networks operating across Central America during the last decades have been added to create a single dataset of recordings from

subduction events until 2006. The subduction recordings for the period 1996-2006 have been contributed by the SNET and UCA networks in El Salvador (148 and 206 records, respectively), the INETER network in Nicaragua (94 records), and the CONRED network in Guatemala (20 records). The final database consists of 554 triaxial ground-motion recordings from subduction events of moment magnitudes between 5.0 and 7.7 at distances from about 20 to 400 km.

As observed in Figure 3 and Figure 4, which provide an overview of the distribution of the dataset, the magnitude range of the intraslab dataset for Central America has been extended by the inclusion of the recordings from the 13 January 2001 (M_W 7.7) El Salvador event. In addition, 295 new recordings from intraslab events of magnitudes $5.0 \leq M_W \leq 6.6$ have also been added to complement the earlier data in this magnitude range. The interface data have similarly been supplemented by the inclusion of 109 new recordings, 45 of which are from interface events of magnitudes $6.0 \leq M_W \leq 6.9$. The interface database has also been extended in terms of distance coverage by the addition of 30 new recordings from distances less than 100 km. It is noted, however, that the largest interface event in the database is the 25 March 1990 M_W 7.3 (HRV) Costa Rican event and no larger interface events have been recorded in this region since. Table 1 summarises the characteristics of the entire (1976-2006) subduction database. Note that the reported number of interface and intraslab records from each country corresponds to the number of data recorded by the networks in that particular country – including events that occurred in other countries – and not only the number of records associated to events that occurred within the borders of that particular country. Most of the new data, a large number of which are from the 2001 earthquake sequence, have been recorded by the UCA and SNET (formerly CIG) networks in El Salvador. New data from Nicaragua have also been made available, although many of the records are from small-to-moderate magnitude events (M_W=6.0) recorded at long distances (R_{rup}>100 km) and consequently have relatively low amplitude (PGA<50 cm/s^2). Data from two recent subduction events in Guatemala have also been added (15 records).

In the following sections, the steps taken during the compilation of this database are described in greater detail, including: evaluation of the earthquake-related parameters (*i.e.*, magnitude, location, fault mechanism, fault size and orientation); classification of subduction events by type (*i.e.*, interface or intraslab); computation of source-to-site

distance metrics; characterisation of site conditions at recording stations using different parameters (*i.e.*, surface geology descriptors, shear-wave velocity profiles, natural site period and normalised response spectra shapes) and assignation of site classes following various classification schemes (*i.e.,* NEHRP classification, the New Zealand site classification scheme used by McVerry *et al.,* 2006 and the scheme used by Zhao *et al.,* 2006). The metadata listed in the Douglas *et al.* (2004) database has also been reviewed and completed during this study. Earthquake source parameters have been re-assessed, additional source-to-site distances have been computed for finite-source distance metrics and further data on the site conditions have been included.

3.1 Documentation of events and data selection

Before defining the data selection criteria, it was first necessary to identify subduction records. The strong-motion records for the period 1996-2006 had not been documented and hence no information on the type of causative earthquake (*i.e.*, shallow-crustal or subduction) was released by the network operators with the data. A systematic search for source parameters in the International Seismological Centre (ISC) catalogue and the recently available EHB Bulletin was carried out in order to establish whether the recordings were from an upper-crustal or subduction-type event, and a preliminary set of data was selected on the basis of hypocentral locations. Recordings from subduction events included in the Douglas *et al.* (2004) database were also selected on this basis.

In selecting the data, a minimum magnitude level of M_W 5 was specified, which is the minimum magnitude value for which Centroid Moment Tensor (CMT) determinations are reported in the Harvard CMT catalogue. This magnitude cut-off was required as CMT determinations are an essential input for the classification of subduction events (*i.e.*, interface or intraslab) on the basis of their rupture mechanism. Although this data-selection criterion was driven by metadata availability, the peak acceleration levels of recordings from the subduction events with M_W<5.0 were all less than 20 cm/sec^2 and hence they had little engineering significance. It is noted that 6 recordings from events prior to 1976, for which no CMT determinations were available, have been excluded from the database. The excluded records were from four events of magnitude M_L less than 5.4 and had peak amplitudes less than 10 cm/s^2.

From this preliminary dataset of recordings from subduction events with M_W=5.0, only records with a minimum peak acceleration level of 1 cm/sec^2 were selected. No maximum source-to-site distance was specified although in practical terms this is controlled by the minimum peak acceleration level. All selected data have been recorded by free-field and structure-related free-field instruments (*i.e.*, instruments located on the ground floor or in the basement of structures up to three storeys in height). Recordings from instruments located in the lower levels of buildings of more than 3 storeys have been collected but excluded from the analyses. The final dataset consists of 554 triaxial ground-motion recordings from both interface and intraslab events that occurred along the Central American subduction zone between 1976 and 2006. Of these, 111 triaxial ground-motion recordings from 32 subduction-type earthquakes and 54 stations in Costa Rica, El Salvador and Nicaragua, had previously been included in the Douglas *et al.* (2004) database (1976-1996). The more recent database compiled herein (1996-2006), consists of 443 triaxial strong-motion records from 53 subduction-type events and 56 stations in El Salvador, Nicaragua and Guatemala.

The earthquake information compiled for each subduction event in the database consists of event date, epicentral location, focal depth, earthquake magnitude in various scales and rupture mechanism. Epicentral locations and depths of earthquakes along the Middle American Trench were obtained from the online catalogue of the US Geological Survey's National Earthquake Information Centre (NEIC) and the ISC and EHB Bulletins. Regional determinations reported by the Geotechnical Investigation Centre (CIG) and the Central American Seismic Centre (CASC) were also used in this study when available. In addition to the above sources of information, locations from detailed regional seismicity studies such as that of Ambraseys & Adams (2001) and from special studies with accurate relocations (*e.g.*, Protti *et al.*, 1995; Warren *et al.*, 2008; Vallée *et al.*, 2003) were included. Surface-wave magnitude (M_S) and body-wave magnitude (m_b) values reported by international agencies (*i.e.*, ISC and NEIC) and regional agencies (*i.e.*, CIG and CASC) are also listed. The moment magnitude (M_W) estimate and focal mechanism solution for each event, as retrieved from the Harvard CMT database are also included alongside the corresponding style-of-faulting classification. For the latter, the Frohlich & Apperson (1992) scheme based on principal stress axes orientation has been used in addition to the Wells & Coppersmith (1994) scheme based on rake angles. Summary pages including a complete listing of the source parameters of the Central American earthquakes considered

in the present study are presented in Arango (2010); a catalogue with the final determinations of the parameters is provided as an electronic supplement to this paper.

The subduction events were classified by type (*i.e.*, interface or intraslab), on the basis of focal mechanism, epicentral location, depth, and position with respect to trench axis. Focal mechanism solutions were used to identify those events consistent with thrusting along the plate interface and those consistent with normal faulting within the subducted slab. Amongst subduction events, pure reverse-faulting mechanisms are associated with interface events if they occur as thrust faulting on a shallow-dipping focal plane oriented approximately parallel to the local trench axis and at depths less than the maximum depth of the seismically-coupled interface. Along the Middle American Trench, the maximum depth extent of seismically-coupled interface has been found to be ~47 km, as defined by teleseismic locations (*e.g.*, Pacheco *et al.*, 1993), with more detailed studies suggesting that this depth varies between 25 and 35 km along the Costa Rica segment (*e.g.*, Protti *et al.*, 1995; DeShon *et al.*, 2003; DeShon *et al.*, 2006; Hansen *et al.*, 2006). Reverse faulting events not meeting these criteria were considered to be associated with intraslab activity. These included reverse and reverse/strike-slip events below the coupled-plate interface occurring on nodal planes whose orientation and dip are incompatible with the geometry of the interface (*i.e.*, planes non-parallel to the local trench axis, steeply-dipping planes or a combination of both). Normal faulting mechanisms (or any combination of normal/strike-slip or strike-slip/normal) are always associated with activity within the slab (intraslab-type events), occurring below the plate interface.

To address the classification of subduction events, it was first necessary to establish which of the earthquake catalogues would provide the best epicentral locations and focal depths. Therefore, the various hypocentral determinations were plotted against the subducted slab geometry as given by the cross-sections of seismicity constructed in Figure 1. For earthquakes along the Nicaraguan and Costa Rican segments, the slab geometry mapped by Syracuse *et al.* (2008) using seismic tomography profiles was also considered. A preferred earthquake location was then selected as the one being most consistent with the depth extent of the mapped seismically-coupled plate interface and the characteristics of faulting observed at different depths. For instance, one would expect the reported depth for an event with focal mechanism consistent with thrust faulting along the plate interface to be above the maximum depth extent of the mapped coupled interface in the region.

Similarly, the reported location of a normal-faulting event should place the event within the slab and below the coupled plate interface.

It was found that the depths of Central American events reported in the ISC Bulletin, some of which have been used by Ambraseys & Adams (2001), placed events with focal mechanisms consistent with interface events well below the mapped interplate contact in the region (35-50 km). It was also noted that there were important differences between the depth estimates reported in the ISC and EHB Bulletins, with the depths in the former being generally greater than those listed in the EHB Bulletin. As shown in Figure 5, the epicentral locations reported in the ISC and EHB Bulletins for the Central American events used in this study are fairly similar, with horizontal distances perpendicularly to the trench (D_{trench}) all less than 20 km, but the ISC depths are up to 60 km greater than those reported in the EHB Bulletin. Large errors of overestimation in ISC focal depths for earthquakes in this particular region have been identified previously (*e.g.*, Ambraseys *et al.,* 2001). These differences in depth are probably due to differences in the velocity models used as the determinations in the EHB Bulletin are based on the same phase data as used by ISC. Similarly, the CMT centroids were systematically located closer to the trench than the reported hypocentres, even though one would expect the centroid to be close to the hypocentre location given the magnitude of most of these events (M_W<6.0). After a detailed examination of each reported location it was decided that the EHB Bulletin provides the most consistent hypocentre determinations. It is noted that in cases where the EHB reported depth was fixed, the location from regional agencies was chosen as the preferred input. Similarly, when locations from detailed studies of aftershock sequences were available those locations were used instead of the ones reported in the EHB Bulletin.

The general criteria for classifying events as interface were as follows: a pure reverse or predominantly reverse fault mechanism following the Wells & Coppersmith (1994) scheme with fault plane approximately parallel to the local trench axis dipping less than about 25º (allowing for a 10° variation in the dip). A value of 50±10 km for the maximum depth of nucleation of thrust events was assumed along the Guatemala-Nicaragua segment and 35±10 km for the Costa Rican segment. These values were selected on the basis of the depth of the seismically coupled zone mapped along Central America, and the maximum errors associated with the EHB depth determinations. A value of 25º±10º was chosen for the maximum dip angle of the fault plane orientated in the trench direction based on the

dip of the Cocos slab at shallow depths (20º-30º). These criteria are similar to those used in other studies (Tichelaar & Ruff, 1993; Bilek & Lay, 1999). In a small number of cases reverse-mechanism events consistent with thrust faulting along the plate interface were placed at depths greater than the maximum depth of nucleation of thrust events estimated by Pacheco *et al*. (1993). These events occurred along the Guatemala segment (*i.e.*, the 27 October 1979 14:35 and 21:43 Guatemala events) at depths shallower than 65 km (EHB) and less than 125 km from the trench. Since no detailed information as to the geometry of the seismogenic zone in this particular segment is available to determine whether the events actually occurred on the interface, it was assumed that they are related to interface activity on the basis of their fault mechanism and their position along the slab (~125 km from the trench).

The general criteria for classifying events as intraslab were as follows: a normal mechanism, following the Frohlich & Apperson (1992) scheme, or a reverse mechanism with source depths greater than about 50 km occurring on planes that are incompatible with the orientation of the trench and the slab dip along the plate interface. For instance, reverse events with one nodal plane trending semi-parallel to the trench axis but with a steep-dip angle were classified as intraslab. It should be noted that even if the conjugate plane is shallow dipping, its dip and orientation may be incompatible with the geometry of the interface.

In addition, reverse-mechanism events on shallow-dipping planes occurring within the slab at depths greater than 100 km were also classified as intraslab in agreement with fault plane orientations of intermediate-depth events determined by Warren *et al.* (2008) along the Middle American Trench. Any other combination of strike-slip and either normal or reverse mechanism, corresponding to the "odd" category of Frohlich & Apperson (1992), occurring at depths greater than ~50 km and at >150 km from the trench, were also classified as intraslab events (*i.e.*, the 20 July 1978 Nicaragua and the 29 April 1983 El Salvador events). It is noted that the seismic activity recorded offshore El Salvador during 2001, following the 13 January 2001 (M_W 7.7) earthquake event, was classified as occurring within the slab or along the interface based on the relative position of each aftershock with respect to the fault plane geometry of the mainshock.

In total, 80 subduction-type events that occurred along the Middle American Trench during the period 1976-2006 were classified using the above criteria. The locations of the events listed in the Douglas *et al.* (2004) database were also re-assessed and the classification by source type was extended to these earlier events in order to ensure consistency. Overall, 24 events correspond to interface and 56 correspond to intraslab-type events. The locations of the subduction events used in this study are shown in Figure 6 alongside the moment magnitude and focal mechanisms of M_W=6.0 events. Many of the events classified as intraslab, most of which are associated with the 2001 sequence, are located near the coast of El Salvador. Intraslab events are also concentrated along the Guatemalan and Nicaraguan segments of the subduction zone. Finally, it is noted that the majority of the events recorded in Costa Rica are interface-type events of intermediate-to-large magnitude. The larger proportion of interface events in this region is consistent with studies that suggest a much stronger seismic coupling along the Costa Rican segment of the Middle American Trench (Protti *et al.*, 1995).

3.2 Record processing

Strong-motion records from the Douglas *et al.* (2004) database are available in a processed format and therefore no processing of these waveforms was performed, although quality assurance was undertaken for all selected data by visually inspecting the acceleration, velocity and displacement time series of each record and re-computing the corresponding elastic response spectra. It is noted, however, that standard low-cut (0.25 Hz) and high-cut (25 Hz) filters were applied to all acceleration traces in the Douglas *et al.* (2004) database, and therefore the spectral ordinates may only be reliably calculated up to 3 seconds (*e.g.*, Akkar & Bommer, 2006). Processing of the more recent dataset (1996-2006), has been performed in a similar manner to that described in Arango *et al.* (2010) for the Peruvian-Chilean dataset. Most of the data contributed by the UCA and CONRED networks have only been released in a processed format and hence solely a visual inspection of these waveforms and computation of elastic response and Fourier amplitude spectra have been possible. Ground-motion records available in an unprocessed format were processed using the TSPP collection of FORTRAN programs for processing and manipulating time series, developed by Dr David Boore from the US Geological Survey (Boore, 2008).

Before applying any filtering procedure, an initial baseline adjustment was applied to the accelerograms (zeroth-order correction). The mean determined from the pre-event portion of the record, or the mean computed from the whole record if the pre-event portion was not available, was subtracted from the entire acceleration time series. After making this initial baseline correction, the acceleration traces were integrated, without filtering, to check for long-period drifts that could indicate the presence of offsets in the reference baseline. In most cases baseline offsets were small and the long-period noise was removed by filtering. The records were then filtered using an acausal bidirectional 8th-order Butterworth filter. For those records with adequate pre-event memory, the low-cut filter frequencies were estimated from consideration of the signal-to-noise ratio of each channel, compared to the model of the noise obtained from the pre-event memory. However, the majority of the time-histories available from digital instruments did not include pre-event portions of sufficient length to estimate the noise and therefore visual inspection of the velocity and displacement traces was used as the basis for the selection of the low-cut filter frequency. For those records with adequate pre-event memory, the low-cut filter frequencies were estimated from consideration of the signal-to-noise ratio between each channel and the model of the noise obtained from the pre-event memory.

For the analogue recordings included in the dataset, low-cut filter frequencies were selected based on comparison of the Fourier Amplitude Spectrum (FAS) of the record with the noise spectra proposed by Lee and Trifunac (1990) and Skarlatoudis *et al.* (2003). Since these models of noise may be biased as they correspond to a particular combination of accelerograph and digitiser, which does not necessarily match that of data being processed, visual examination of the velocity and displacement traces was also used as criterion for the selection of the low-cut filter frequency. Finally, removal of high-frequency noise was achieved by using high cut-off filters at 25 Hz for records from analogue instruments and 50 Hz for records from digital instruments. Peak values of the velocity and acceleration response spectral ordinates for 5% of the critical damping were then obtained from the processed data. The maximum usable period of each spectrum was defined as 0.8 times the low-cut filter period following Abrahamson and Silva (1997). On this basis it was decided that for all records included in the database, the spectral ordinates could be confidently calculated up to 3 seconds, although the usable period range could easily be extended up to 4 seconds or longer for most of the digital records.

3.3 Source-to-site distances

The source-to-site distance for each record was characterised in terms of the closest distance to the earthquake fault plane or rupture distance (R_{rup}). Fault plane geometries from published finite-source models based on wave-form inversion were, however, only available for the 13 January 2001 (M_W 7.7) El Salvador earthquake, for which rupture distances were computed based on the Vallée *et al.* (2003) source model. For the 19 June 1982 (M_W 7.3) event the fault plane geometry and orientation used was that estimated by Martínez-Díaz *et al.* (2004) for their stress transfer modelling for this event. For the 25 March 1990 (M_W 7.3) Costa Rica earthquake, the dimensions of the rupture were constrained using the distribution of 1-day aftershocks reported by Protti *et al.* (1995). The fault plane was modelled using a strike of 298° and dip angle of 26° indicated by the focal mechanism determined by Protti *et al.* (1995), which was considered to be consistent with the trench-axis orientation and dip angle of the Cocos slab in this region. These three earthquakes are the only events with magnitude M_W>7.0 included in the database.

For those events of unknown geometry, the same alternative approach described in Arango *et al.* (2010) was used to estimate the fault plane-related distance metrics. Rupture areas were estimated from empirical relationships between source dimensions and moment magnitude (M_W) for interface and intraslab-type events determined by Strasser *et al.* (2010). The fault planes were located in space, assuming that the epicentre lies above the centre of the dipping plane. The orientation and dip angle for interface events was chosen from the two sets of angles listed in the Harvard CMT catalogue, as the one being more consistent with the geometry of the subduction zone (*i.e.,* strike parallel to the local trench axis and dip approximately <30º). The fault plane orientations of the intraslab events along the Middle American Trench identified by Warren *et al.* (2008) were also used for the estimation of rupture distances. For intraslab events with no identifiable fault plane orientation, the distances to each of the two focal planes reported in the CMT catalogue were computed and the geometric mean of these two values was used as an estimate of the rupture distance. This procedure was used for M_W=6.5 events recorded at distances less than 100 km from the hypocentre and only for three events with magnitude 6.0≤M_W=6.5 recorded at distances beyond. The general approach used is expected to provide a reasonable approximation for the purpose of source-to-site distance calculations, in particular for M_W=6.5 events, for which the Strasser *et al.* (2010) scaling relations for

subduction events predict source areas greater than 400 km^2 and hence estimating the difference between rupture and hypocentral distances becomes non-trivial. For smaller events the hypocentral distance was assumed to be equal to the rupture distance as their fault dimensions are not likely to be very large compared to the source-to-site distances.

3.4 Recording station information and assignment of site classifications

Site conditions were evaluated for 110 stations located in Guatemala, El Salvador, Nicaragua and Costa Rica and site classes were assigned following various site classification schemes, including the widely-used NEHRP site classification method (NEHRP, 1997), the New Zealand classification scheme used by McVerry *et al.* (2006), and the scheme used by Zhao *et al.* (2006). It is noted that very limited geotechnical information was available in order to make direct assignations of site classes and shear-wave velocity (V_S) profiles were only available for 5% of the stations used in this study. Consequently, the assignment of site classes was generally based on a combination of the following indicators: geological characteristics of the sites as interpreted from geological maps or as reported in previous studies, V_S profiles at recording stations, when available; predominant site periods from published site-response studies carried at some of the stations, and site classes assigned by previous studies. Site conditions were also evaluated from spectral ratios between horizontal and vertical components of earthquake recordings (*e.g.*, Lermo & Chávez-García, 1993; Field & Jacob, 1995; Atakan, 1995; Zaré *et al.*, 1999; Rodriguez & Midorikawa, 2003; Zhao *et al.*, 2006; Haghshenas *et al.*, 2008) and from normalised spectral shapes (SA/PGA). Additionally, site conditions were evaluated from down-hole arrays as well as from soil-to-rock spectral ratios for sites sufficiently close to one another.

The horizontal-to-vertical ratios of FAS were computed for each station, using a dataset of ground motions from subduction-zone events of magnitudes $5.0 \leq M_W \leq 6.9$ recorded at distances $R_{rup} \leq 75$ km. Low-amplitude acceleration records (PGA<100 cm/s^2) were preferred to records of strong motion in order to ensure that the estimated site periods are not shifted significantly as a result of non-linear effects. At some sites, however, no weak-motion records were available and therefore the estimated site response is most likely non-linear. FAS were computed for each component and smoothed with the Konno and Ohmachi smoothing function (Konno & Ohmachi, 1998), using the “smc2fs2.exe” utility

developed by Boore (2008). For each station, the site period was then calculated by considering the spectral ratios between the smoothed horizontal components and the smoothed vertical component of each record.

The H/V ratios computed from ground-motion records have been used only as a guide in the assignment of site classes, by considering the period band over which the ground motion is amplified, and not as a direct input in site classifications based on the site period, such as the Zhao *et al.* (2006) scheme derived for stations in Japan, since at many stations few recordings were available to check the stability of the computed ratios. More detailed analyses of local site effects at the Central American stations are beyond of the scope of this work.

Table 2 lists the geological and geotechnical information on the stations operated by the CIG, SNET and UCA networks in El Salvador. For the stations of the no longer operational CIG analogue network, the description of the surface geology was obtained from Cepeda *et al.* (2004) and Douglas *et al.* (2004). Information on the surface geology at the stations of the SNET digital network was obtained from Climent *et al.* (2007) and from the digital version of the geological map of El Salvador available at the SNET website (http://mapas.snet.gob.sv/). For the stations of the UCA network the information has been taken from Cepeda *et al.* (2004) and from the accelerogram headers, when available. The V_{S30} values calculated from the Faccioli *et al.* (1988) profiles at the UC, CI, IG, and HSH stations are also listed, along with the predominant site periods, as interpreted from the site-amplification spectra determined by Salazar *et al.* (2007) using inversion analysis as well as reference-site and H/V spectral ratios from records. The H/V ratios computed herein are also listed in these tables, although it is noted that for stations with a limited number of records (one or two) the site periods from published studies (*e.g.*, Salazar *et al.*, 2007), were the preferred input used for the site-classes assignment.

Many accelerograph stations in El Salvador are concentrated along the volcanic chain and in San Salvador city. The San Salvador area is underlain by Quaternary volcanic and volcanoclastic deposits mainly derived from adjacent volcanoes. Of relevance to site response analyses, there are two main deposits constituting the San Salvador Formation, which covers the area of San Salvador city. These are the younger volcanic ash, locally known as "*tierra blanca*" (Rolo *et al.*, 2004) and the underlying brown-coloured Pleistocene

tuffs (Schmidt-Thomé, 1975). The "*tierra blanca*" deposits are originated from multiple eruptions of the former Ilopango volcano and their thickness varies significantly, reaching up to 25 m underneath the city and 50 m towards the Ilopango lake (Rymer, 1987). The tuff deposits are slightly older and more consolidated material derived from the San Salvador volcano and may reach thicknesses of up to 25 m. The characteristics of this 10-30 m thick layer of sediments are largely variable along San Salvador, exhibiting varying levels of consolidation (Atakan *et al.*, 2004). The presence of thick volcanoclastics makes this area prone to amplification of seismic waves, as discussed in previous studies of site effects within volcanic deposits in San Salvador (*e.g.*, Atakan *et al.*, 2004; Faccioli *et al.*, 1988, Salazar *et al.*, 2007).

These volcanic deposits generally have an average shear-wave velocity between 200-300 m/s over the top 30 m (Faccioli *et al.*, 1988), and therefore stations on these materials have been classified as NEHRP site class D and D/E. Figure 7 shows the H/V ratios of Fourier spectra calculated for various stations of the UCA and SNET digital networks. As seen in this figure, stations on volcanic deposits (ESJO, UDBS, UESS, SNET and CSBR) are associated with amplification at periods longer than 0.4 sec. The amplification towards longer periods observed at CSBR station may be related to thickness of the volcanic ash ("*tierra blanca*") at this site, which extends up to about 25 m depth (Salazar *et al.*, 2007). It is noted that the ability of the H/V ratios to reveal resonance periods depends on the velocity contrast between the stratigraphic layers, as in the case of soft deposits underlain by rock or much stiffer sediments, and that this technique is less efficient on stiff, thick soil deposits (Rodríguez & Midorikawa, 2003; Haghshenas *et al.*, 2008).

The USPN station is situated on volcanoclastics over welded tuffs, on the crest of a ridge orientated in the EW direction, and hence large amplitudes at longer periods (~1.0 sec) may be related to a topographic effect. Recording stations in El Salvador are also distributed across the country on different geologies. For instance, the AIES, HERR, ULLB, SMIG, and SONS sites are located on sedimentary deposits, consisting of alluvial materials intercalated with pyroclastics, which are found in the southern part of the coastal region and in the coastal plains in the western and central part of El Salvador. The H/V ratios and spectral shapes for the ULLB station indicate a clear predominant period of less than about 0.2 sec, which is consistent with a relatively thin layer (~10m) of alluvial-type materials overlying bedrock (lavas). Only five stations (UPAN, ACAJ, QC, CU, and CM)

have been classified as on rock or soft rock, corresponding to NEHRP site class B, although there may well be thin soil cover at these sites, which is not reported on geological maps due to their spatial resolution. Geophysical data at the UPAN station indicate hard rock with V_S~2,100 m/s (Faccioli *et al.*, 1988). Three more stations are located on volcanic deposits overlying lava flows (CI, HSH and SE), which have been classified as NEHRP site class C. V_S profiles at the CI and HSH sites indicate a V_{S30} values of approximately 550 m/s, with an upper layer of soil about 7 m in thickness (Faccioli *et al.*, 1988). Other hard soil sites have also been classified as NEHRP site class C on the basis of the H/V ratios and SA/PGA shapes, as in the case of the HSRF station which is andesitic and basaltic materials.

Table 3 lists the information on the stations in Nicaragua used for the assignment of site classes. The general geological characteristics of Nicaraguan sites presented in these tables are interpreted from the 1:500,000 geological map of Nicaragua (INETER, 1995) and the 1:50,000 geological map of Managua (INETER, 2003). For the stations of the IIS network that are no longer in operation, the site conditions assigned in previous studies (*e.g.*, Segura *et al.*, 1994) are also listed. The V_{S30} values calculated from the V_S profiles reported by Faccioli *et al.* (1973) for the ESSO refinery station and by Parrales & Picado (2001) for the Managua, Teatro Nacional station are listed along with the site periods calculated from H/V Fourier spectra ratios.

The accelerographic stations in Nicaragua are situated on diverse geologies: the Jinotega, Jinotepe and Boaco sites are situated in the Interior Highlands, on Tertiary volcanic rocks and have been classified as NEHRP site class B. The Rivas site lies on the Pacific coastal plain on stiff marine sediments, classified as NEHRP class C. The stations located in the towns of Chinandenga, León and Corinto are located on alluvial-type materials and have been classified as NEHRP sites D and D/E on the basis of the H/V ratios and spectral shapes. The remaining stations are located in the Managua area, in the middle of the Nicaraguan depression. The soils across Managua consist of a volcano-sedimentary sequence, based in the Sierras group, overlain by pyroclastic materials from the Holocene which form the Las Nubes and Managua groups (Hradecky *et al.*, 1997). In general, the soils in Managua can be classified as non-cohesive silts, sands and gravels, with different levels of consolidation and cementation, forming a sequence that extends down to a maximum depth of about 15 m. The basement, the Sierras group, consists of volcanic tuff

and is found at depths as shallow as 510 m (Parrales, 2006). Previous studies have determined shear-wave velocity profiles within the soils underlying Managua (*e.g.*, Faccioli *et al.*, 1973; Parrales, 2006). The latter study determined shear-wave velocity profiles at several locations across Managua city, and found that the depth to soft rock, defined as material with $360 < V_S < 760$ m/s, varies from 8.5 to 16 m. This material is related to Las Sierras group, which is overlain by stiff soils with $180 < V_S < 360$ m/s and thicknesses between 6 and 13 m. Soft soils with a $V_S < 180$ m/s occur in the first 1.5 to 3 m in depth. The V_s profile for the ESSO refinery station in Managua (RAAN) indicates a value of $V_{S30} = 290$ m/s, and hence this site is classified as NEHRP class D. The other stations in Managua used in this study have been classified as NEHRP site class C/D and D, and have site periods generally less than 0.5 sec, based on the H/V ratios calculated herein from accelerographic recordings.

Table 4 lists the information on the stations in Costa Rica used for the assignment of site classes. The general geological characteristics of Costa Rican sites presented in these tables are taken from Climent *et al.* (1992), Taylor *et al.* (1994), EERI (1991), Douglas *et al.* (2004) and Climent *et al.* (2007). The predominant site periods, as interpreted from the site-amplification spectra determined by Moya (2009), at several stations of the LIS accelerometric network are also listed along with those calculated herein from H/V Fourier spectra ratios of recorded ground motions. It is noted that no shear-wave velocity profiles at the Costa Rican sites have been made available and hence the assignments of site classes were generally based on the normalised spectral shapes and the H/V ratios, in combination with the other information available.

The strong-motion stations of the LIS network used in this study are mainly located in the Central Valley region and along the Pacific coast. Most of the stations are concentrated in the Central Valley, in the cities of San José, Cartago, Alajuela and San Ramón. The stations in San José city are situated on volcanic rocks (lahar) overlain by volcanic ash. The thickness of volcanic sediments above the lahar in the San José area may reach up to 35 m, being deeper in the northern part of San José and shallower in the southern part (Moya *et al.*, 2000). The predominant site periods in some areas of San José reported by previous studies (Moya *et al.*, 2000) approximately correlate with the thickness of the sediments, with sites to the north of the area exhibiting amplifications towards longer periods. For instance, the ECA station is situated on volcanic sediments of about 20 m

depth, underlain by lahars and shows amplification at periods of about 0.5 sec (Moya, 2009). Similarly, the HTO site is situated in the San José area on deposits of about 10 m depth and shows amplification at periods of about 0.4 sec. The ALJ station in the city of Alajuela lies on soft volcanic sediments and the H/V ratios are associated with large amplifications at periods of about 0.9 sec. The ISD and GLF stations are situated on hard sediments and are associated with site periods less than 0.45 sec (Moya, 2009). The CTG station is located in the city of Cartago, on soft sediments within an alluvial valley. The APBO, APQS, APSA, APSD, CCH, ALCR stations lie on volcanic or sedimentary rocks, some of which are overlain by a soil cover and are associated with low amplifications.

Table 5 lists the information used for the assignment of site classes for the stations in Guatemala. The general geological characteristics of Guatemalan sites presented in these tables have been provided by the network operator (CONRED), and have been interpreted from the 1:250,000 geological map of Guatemala (IGN, 1993). Surface geology descriptors have also been taken from Climent *et al.* (2007). It is noted that no V_S profiles at the recording stations have been made available and hence the assignment of site classes was based on the surface geology descriptors in combination with the normalised spectral shapes and the H/V ratios. The stations used in this study are installed within the urban limits of Guatemala City and at the southwestern side of the city. The area surrounding Guatemala City is a graben controlled in the north by major strike-slip faults constituting the Motagua-Polochic Fault system. The area of the city is mostly covered by pumice, derived from the Quaternary volcanoes. The youngest sediments in the region are alluvial deposits which are attached to the drainage system joining the Amatitlán Lake. There are two main deposits of relevance to local site response: the Quaternary pumice deposits, consisting of ash and pumice with depths exceeding 60 m, and the Quaternary alluvia with more than 15 m thickness and characterised by shear-wave velocities of about 150 m/s (Ligorría & Atakan, 1997). The geological site conditions at the stations of the CONRED network vary from thick pyroclastic deposits to recent alluvial deposits. Only one instrument was installed on a rock outcrop site (TNG), but no earthquake recordings from this station are included in this study. The EPRG and EPQG stations lie on soft alluvial deposits and have been classified as NEHRP site class D and D/E. The GEG and MPG sites are situated to the south of the Amatitlán Lake on lahars and alluvium, and have been classified as NEHRP D on the basis of their spectral shapes. The PECG, IGSS, and HSMG stations are situated on Quaternary pumice deposits and have been identified as

hard soil (Climent *et al.*, 2007). Spectral shapes at these sites are associated with low amplification and they have consequently been classified as NEHRP site C and C/D.

4. CONCLUSIONS

A database of recordings from subduction-zone earthquakes in Central America and associated information has been compiled, with emphasis on the quality of both the records and the associated metadata. Although the database presented in this study is not sufficient in terms of magnitude-distance coverage to serve as a basis for the derivation of predictive equations for interface and intraslab events in Central America, it considerably expands the Central American subduction data compiled in previous studies and used in early ground-motion prediction studies for subduction events in this region (*e.g.*, Schmidt *et al.*, 1997). The compiled database further adds to the global strong-motion data that can be used in the derivation of global predictive equations for subduction environments (*e.g.*, Youngs *et al.*, 1997; Atkinson & Boore, 2003; 2008). Finally, the compiled database will allow the assessment of the existing predictive models for subduction-type events in terms of their applicability to Central America, which is essential for an adequate estimation of subduction-related hazard in this region.

ACKNOWLEDGEMENTS

The doctoral research of the first author, on which this paper is based, has been partially funded by the Alßan Programme of the European Union under scholarship E05D053967CO and the COLFUTURO programme; their financial support is gratefully acknowledged. The authors would like to thank to the following organisations and agencies for providing the strong-motion records used in the present study: The National Service of Territorial Studies of El Salvador (SNET), the Central American University (UCA), the Nicaraguan Institute of Territorial Studies (INETER) and the National Commission for Disaster Reduction (CONRED) of Guatemala. Thanks are extended to J Douglas, H. Bungum, A. Dahle, C. Lindholm, A. Climent, W. Taylor Castillo, P. Santos Lopez, V. Schmidt, and W. Strauch for providing the Central American strong-motion database for the period 1966-1996. We are extremely grateful to David Boore and two anonymous reviewers, whose detailed and insightful reviews led to considerable improvements of the manuscript.

REFERENCES

Abrahamson, N. A.& W.J. Silva (1997). Empirical response spectral attenuation relations for shallow crustal earthquakes. *Seismological Research Letters* **68**(1),94–127

Akkar, S. & J.J. Bommer (2006). Influence of long-period filter cut-off on elastic spectral displacements. *Earthquake Engineering & Structural Dynamics* **35**(9), 1145-1165.

Ambraseys, N.N., and R.D. Adams (2001). *The seismicity of Central America. A descriptive catalogue 1898-1995.* Imperial College Press, London, 309 pp.

Ambraseys, N.N., J.J. Bommer, E. Buforn & A. Udías (2001). The earthquake sequence of May 1951 at Jucuapa, El Salvador. *Journal of Seismology* **5**(1), 23-39.

Arango, M.C. (2010). Ground-motion prediction for subduction-zone earthquakes: Insights from South And Central American Data. *PhD Thesis*, Imperial College London.

Arango, M.C., F.O. Strasser, J.J. Bommer, R. Boroschek, D. Comte and H. Tavera (2010). A strong-motion database from the Peru-Chile subduction zone. *Journal of Seismology*, in press, doi: 10.1007/s10950-010-9203-x.

Atakan, K.(1995). A review of the type of data and techniques used in the empirical estimation of local site response. *Proceedings of the 5th International Conference on Seismic Zonation*, Nice, France, 17-19 October 1995, Vol. II, p. 1451-1460.

Atakan, K., M. Ciudad Real, and R. Torres (2004). Local site effects on microtremors, weak and strong ground motion in San Salvador, El Salvador. In: Rose, W.I., J.J. Bommer, D.L. López, M.J. Carr, and J.J. Major (eds), *Special Paper 375: Natural hazards in El Salvador*, Geological Society of America, Boulder, Colorado, p.321-338.

Atkinson, G.M., and D.M. Boore (2003). Empirical ground-motion relations for subduction-zone earthquakes and their application to Cascadia and other regions. *Bulletin of the Seismological Society of America* **93**(4), 1703-1729.

Atkinson, G.M., and D.M. Boore (2008). Erratum to: Empirical ground-motion relations for subduction-zone earthquakes and their application to Cascadia and other regions. *Bulletin of the Seismological Society of America* **98**(4), 2567-2569.

Benito Oterino, M.B. and Y. Torres Fernández (*eds*) (2009). Amenaza Sísmica en América Central. Entimema, Madrid, 371 pp.

Bilek, S.L. and T. Lay (1999). Comparison of depth dependent fault zone properties in the Japan Trench and Middle America Trench. *Pure and Applied Geophysics* **154**(3-4), 433-456.

Bommer, J.J., A. Udías, J.M., Cepeda, J.C. Hasbun, W.M. Salazar, A. Suárez, N. N. Ambraseys, E. Buforn, J. Cortina, R. Madariaga, P. Méndez, J. Mezcua, and D. Papastamatiou (1997). A new digital accelerograph network for El Salvador, *Seismological Research Letters* **68,** 426–437.

Bommer, J.J. & C.E. Rodríguez (2002). Earthquake-induced landslides in Central America. *Engineering Geology* **63**(3/4), 189-220.

Bommer, J.J., M.B. Benito, M. Ciudad-Real, A. Lemoine, M.A Lopez-Menjivar, R. Madariaga, J. Mankelow, P. Mendez de Hasbun, W. Murphy, M. Nieto-Lovo, C.E. Rodriguez-Pineda, and H. Rosa (2002). The El Salvador earthquakes of January and February 2001: context, characteristics and implications for seismic risk. *Soil Dynamics and Earthquake Engineering* **22**(5), 389-418.

Boore DM (2008) TSPP: A collection of FORTRAN Programs for Processing and Manipulating Time Series. Available online from http://www.daveboore.com/ software_online.htm. Last accessed December 2009

Cepeda, J.M., M.B. Benito, and E.A. Burgos (2004). Strong-motion characteristics of January and February 2001 earthquakes in El Salvador. In: Rose, W.I., J.J. Bommer, D.L. López, M.J. Carr, and J.J. Major (eds), Special Paper 375: Natural hazards in El Salvador, Geological Society of America, Boulder, Colorado, p.405-421.

Climent, A., S. Midorikawa, M. Matsuoka, and T. Toshinawa (1992). Processed strong-motion data of near-source accelerograms obtained from Costa Rican Electricity Institute strong-motion network in 1990 and 1991. *DEETEC Report 920207*, Division of Earthquake Engineering, Tokyo Institute of Technology, Tokyo, Japan.

Climent, A., V. Schmidt, D. Hernández, J. Cepeda, E. Camacho, R. Escobar, W. Strauch, and J. Rivas (2007). Strong-motion monitoring. In: Bundschuh, J., and G.E. Alvarado (eds.), *Central America: Geology, Resources and Hazards*, Routledge, New York, Vol.2, Chapter 39.

DeMets, C. (2001). A new estimate for present-day Cocos-Caribbean plate motion: implications for slip along the Central American volcanic arc. *Geophysical Research Letters* **28**(21), 4043-4046.

DeShon, H.R., S.Y. Schwartz, S.L. Bilek, L.M. Dorman, V. Gonzalez, J.M. Protti, E.R. Flueh, and T.H. Dixon (2003). Seismogenic zone structure of the southern Middle America Trench, Costa Rica. *Journal of Geophysical Research* **108**(B10), Article No. B002294.

DeShon, H.R., S.Y. Schwartz, A.V. Newman, V. González, M. Protti, L.M. Dorman, T.H. Dixon, D.E. Sampson, and E.R. Flueh (2006). Seismogenic zone structure beneath the Nicoya Peninsula, Costa Rica, from three-dimensional local earthquake P- and S-wave tomography. *Geophysical Journal International* **164**(1), 109-124.

Douglas, J., H. Bungum, A. Dahle, C. Lindholm, A. Climent, W. Taylor Castillo, P. Santos Lopez, V. Schmidt, and W. Strauch (2004). Dissemination of Central American strong-motion data using Strong-Motion Datascape Navigator. CD-ROM collection, 2004.

EERI (1991). The Costa Rica Earthquake of 22 April 1991– EERI Reconnaissance Report. *Earthquake Spectra* **7**(S2), 1-165.

Engdahl, E.R., R. van der Hilst, and R. Buland (1998). Global teleseismic earthquake relocation with improved travel times and procedures for depth determination. *Bulletin of the Seismological Society of America* **88**(3), 722-743.

Faccioli, E., C. Battistella, P. Alemani, and A. Tibaldi (1988). Seismic microzoning investigations in the metropolitan area of San Salvador, El Salvador, following the destructive earthquake of 10 October 1986. *Proceedings of the International Seminar on Earthquake Engineering*, Innsbruck, Austria, 1988, p. 28-65.

Faccioli, E.E., V. Santayo, and J.L. Leone (1973). Microzonation criteria and seismic response studies for the city of Managua. In: *Proceedings of the Earthquake Engineering Research Institute Conference on the Managua, Nicaragua, Earthquake of December 23, 1972*, Vol. 1,
p. 271–291.

Field, E.H., and K.H. Jacob (1995). Comparison of various site response estimation techniques, including three that are not reference site depending. *Bulletin of the Seismological Society of America* **85**(4), 1127-1142.

Frischbutter, A. (2002). Structure of the Managua Graben, Nicaragua, from remote sensing images. *Geofisica Internacional* **41**(2), 87-102.

Frohlich, C., and K.D. Apperson (1992). Earthquake focal mechanisms, moment tensors, and the consistency of seismic activity near plate boundaries. *Tectonics* **11**(2), 279–296.

Haghshenas, E., P.-Y. Bard, N. Theodulidis, and SESAME WP04 Team (2008). Empirical evaluation of microtremor H/V spectral ratio. *Bulletin of Earthquake Engineering* **6**(1), 75-108.

Hansen, S.E., S.Y. Schwartz, H.R. DeShon, and V. González (2006). Earthquake relocation and focal mechanism determination using waveform cross correlation, Nicoya Peninsula, Costa Rica. *Bulletin of the Seismological Society of America* **96**(3), 1003-1011.

Hradecky, P., P. Hayliceck, M. Navarro, Z. Novak, E. Stanik, and J. Sebesta (1997). Estudio para el reconocimiento de la amenaza geológica en el área de Managua, Nicaragua. *Technical Report*, CGU/INETER, Prague and Managua, 320pp.

Husen, S., E. Kissling, and R. Quintero (2002). Tomographic evidence for a subducted seamount beneath the Gulf of Nicoya, Costa Rica: The cause of the 1990 M_w = 7.0 Gulf of Nicoya earthquake. *Geophysical Research Letters* **29**(8), Article No. L014045.

INETER (1995). 1:500,000 Geological map of Nicaragua, Nicaraguan Institute of Territorial Studies (INETER)

INETER (2003). 1:50,000 Geological map of Managua, Nicaraguan Institute of Territorial Studies (INETER)

IGN (1993).1:500,000 Geological map of Guatemala, National Geographical Institute of Guatemala (IGN)

Kanamori, H. and M. Kikuchi (1993). The 1992 Nicaragua earthquake: a slow tsunami earthquake associated with subducted sediments. *Nature* **361**, 714-716.

Konno, K., and T. Ohmachi (1998). Ground-motion characteristics estimated from spectral ratio between horizontal and vertical components of microtremor. *Bulletin of the Seismological Society of America* **88**(1), 228-241

Lee, V.W., and M.D. Trifunac (1990). Automatic digitization and processing of accelerograms using PC. *Report CE-90-03*, Department of Civil Engineering, University of Southern California, Los Angeles, California, 115pp.

LeFevre L.V., and K.C. McNally (1985). Stress distribution and subduction of aseismic ridges in the Middle America subduction zone. *Journal of Geophysical Research* **90**(B6), 4495-4510.

Lermo, J., and F.J. Chávez-García (1993). Site effect evaluation using spectral ratios with only one station. *Bulletin of the Seismological Society of America* **83**(5), 1574-1594.

Ligorría, J.P., and K. Atakan (1997). Empirical site response estimation in Guatemala City. *Proceedings of the seminar on Assessment and Mitigation of Seismic Risk in the Central American Area*, San Salvador, El Salvador, 22-27 September 1997, p. 141-156.

Martínez-Díaz, J.J., J.A. Álvarez-Gómez, B. Benito, and D. Hernández (2004). Triggering of destructive earthquakes in El Salvador. *Geology* **32**(1), 65-68.

Deleted: [

McVerry, G., J. Zhao, N. Abrahamson, and P. Somerville (2006). New Zealand acceleration response spectrum attenuation relations for crustal and subduction zone earthquakes. *Bulletin of the New Zealand Society for Earthquake Engineering* **39**(1), 1-58.

Moya, A. (2009). Inversión de efectos de sitio y factor Q utilizando cocientes espectrales. *Estudios Geológicos* **65**(1), 67-77.

Moya, A., V. Schmidt, C. Segura, I. Boschini, and K. Atakan (2000). Empirical evaluation of site effects in the metropolitan area of San José, Costa Rica. *Soil Dynamics and Earthquake Engineering* **20**(1-4), 177-185.

NEHRP (1997). Recommended provisions for seismic regulations for new buildings and other structures. *Report FEMA 303*, U.S. Federal Emergency Management Agency, Washington, DC.

Nishenko, S.P.(1989). Circumpacific seismic potential 1989-1999. *Open-File Report 89-86*, U.S. Geological Survey, 126 pp.

Pacheco, J.F., L.R. Sykes, and C.H. Scholz (1993). Nature of seismic coupling along simple plate boundaries of the subduction type. *Journal of Geophysical Research* **98**(B8), 14133-14159.

Parrales, R. (2006). Dynamic soil properties of the soils in the area of Managua, Nicaragua. *Licentiate Thesis in Engineering Geology*. Lund University, Lund, Sweden.

Parrales, R.M., and M.J. Picado (2001). Análisis de espectros de respuesta en el área de la ciudad de Managua. Graduate dissertation, Faculty of Construction Technology, National Engineering University, Managua, Nicaragua.

Protti, M., F. Gündel, and K. McNally (1994). The geometry of the Wadati-Benioff zone under souther Central America and its tectonic significance: results from a high-resolution local seismographic network. *Physics of the Earth and Planetary Interiors* **84**(1-4), 271-287.

Protti, M., K. McNally, J. Pacheco, V. González, C. Montero, J. Segura, J. Brenes, V. Barboza, E. Malavassi, F. Gündel, G. Simila, D. Rojas, A. Velasco, A. Mata, and W. Schillinger (1995). The March 25, 1990 (M_w=7.0, M_L=6.8), earthquake at the entrance of the Nicoya Gulf, Costa Rica: Its prior activity, foreshocks, aftershocks, and triggered seismicity. *Journal of Geophysical Research* **100**(B10), 20345-20358.

Protti, M., F. Güendel, and E. Malavassi (2001). Evaluación del potencial sísmico de la Península de Nicoya, Heredia, Costa Rica, Editorial Fundación UNA, 144 pp.

Rodríguez, V.H.S., and S. Midorikawa (2003). Comparison of spectral ratio techniques for estimation of site effects using microtremor data and earthquake motions recorded at the surface and in boreholes. *Earthquake Engineering and Structural Dynamics* **32**(11), 1691-1714.

Rolo, R., J.J. Bommer, B.F. Houghton, J.W. Vallance, P. Berdousis, C. Mavrommati, and W. Murphy (2004). Geologic and engineering characterization of Tierra Blanca pyroclastic ash deposits. In: Rose, W.I., J.J. Bommer, D.L. López, M.J. Carr, and J.J. Major (eds), Special Paper 375: Natural hazards in El Salvador, Geological Society of America, Boulder, Colorado, p.55-68.

Rymer, M.J. (1987). The San Salvador earthquake of October 10, 1986 – Geologic aspects. *Earthquake Spectra* **3**(3), 435-463.

Salazar, W., V. Sardina, and J. de Cortina (2007). A hybrid inversion technique for the evaluation of source, path, and site effects employing S-wave spectra for subduction and upper-crustal earthquakes in El Salvador. *Bulletin of the Seismological Society of America* **97**(1B), 208-221.

Satake, K. (1995). Linear and nonlinear computations of the 1992 Nicaragua earthquake tsunami. *Pure and Applied Geophysics* **144** (3-4), 455-470

Schmidt V., A. Dahle, and H. Bungum (1997). Costa Rican spectral strong motion attenuation. *Technical Report*, NORSAR, Norway, 1997.

Schmidt-Thomé, M. (1975). The geology in the San Salvador area (El Salvador, Central America), a basis for city development and planning. *Geologisches Jahrbuch* **13**, 207-228.

Segura, F., W. Strauch, W. Taylor, G. Santana, A. Dahle, and H. Bungum (1994). Digital strong motion data from Nicaragua. *Technical Report 2:15*, NORSAR and University of Bergen, Norway, 1994.

Skarlatoudis A, Papazachos C, Margaris B (2003) Determination of noise spectra from strong motion data recorded in Greece. Journal of Seismology 7(4):533–540.

Strasser, F.O., M.C. Arango & J.J. Bommer (2010). Scaling of the source dimensions of interface and intraslab subduction-zone earthquakes with moment magnitude. *Seismological Research Letters* **81**(6), 941-950.

Syracuse, E. M., G. A. Abers, K. Fischer, L. MacKenzie, C. Rychert, M. Protti, V. González, and W. Strauch (2008). Seismic tomography and earthquake locations in the Nicaraguan and Costa Rican upper mantle. Geochemistry Geophysics Geosystems, **9**(7), Article No. Q07S08

Taylor, W., A. Climent, P. Santos, M. Ciudad Real, G. Santana, M. Villagran, W. Strauch, F. Segura, A. Dahle, and H. Bungum (1994). Digital strong motion data from Central America. *Technical Report 2:16*, NORSAR and University of Bergen, Norway, 1994.

Tichelaar, B.W., and L.J. Ruff (1993). Depth of seismic coupling along subduction zones. *Journal of Geophysical Research* **98**(B2), 2017-2037.

Vallée, M., M. Bouchon, and S.Y. Schwartz (2003). The 13 January 2001 El Salvador earthquake: a multidata analysis. *Journal of Geophysical Research* **108**(B4), Article No. B001889.

Warren, L.M., M.L. Langstaff, and P.G. Silver (2008). Fault plane orientations of intermediate-depth earthquakes in the Middle America Trench. *Journal of Geophysical Research* **113**, Article No. B01304.

Wells, D.L., and K.J. Coppersmith (1994). New empirical relationships among magnitude, rupture length, rupture width, rupture area, and surface displacement. *Bulletin of the Seismological Society of America* **84**(4), 974-1002.

Youngs, R.R., S.J. Chiou, W.J. Silva, and J.R. Humphrey (1997). Strong ground motion attenuation relationships for subduction zone earthquakes. *Seismological Research Letters* **68**(1), 58-77.

Zaré, M., P.-Y. Bard & M. Ghafory-Ashtiany (1999). Site characterizations for the Iranian strong motion network. *Soil Dynamics and Earthquake Engineering* **18**(2), 101-123.

Zhao, J., K. Irikura, J. Zhang, Y. Fukushima, P. Somerville, A. Asano, Y. Ohno, T. Oouchi, T. Takahashi, and H. Ogawa (2006). An empirical site-classification method for strong-motion stations in Japan using H/V response spectral ratio. *Bulletin of the Seismological Society of America* **96**(3), 914-925.

TABLES

Table 1: Summary of the interface and intraslab ground-motion data from the Central American subduction zone compiled in the present study, including information on record availability. A flat-file of the compiled database is available as an electronic supplement to this paper.

Table 2: Information on strong-motion stations in El Salvador used in this study.

Table 3: Information on strong-motion stations in Nicaragua used in this study.

Table 4: Information on strong-motion stations in Costa Rica used in this study.

Table 5: Information on strong-motion stations in Guatemala used in this study.

FIGURES

Figure 1: The seismicity of the Central American region, based on the Engdahl-Hilst-Buland (EHB) catalogue for the period 1960-2006. The compiled data database includes subduction events and stations located approximately between latitudes 8-14°N and longitudes 83-92°W. The shallow-focus seismicity associated with volcanism and deformation of the Caribbean plate is not considered in this study. The tectonic setting from Frischbutter (2002) is shown in the upper left graph.

Figure 2: Locations of strong-motion stations contributing data to this study. Data come from the following networks: National Service of Territorial Studies (SNET), Central American University (UCA), Geotechnical Investigation Centre (CIG), Nicaraguan Institute of Territorial Studies (INETER), Seismic Research Institute of Nicaragua (IIS), National Commission for Disaster Reduction (CONRED), Earthquake Engineering Laboratory (LIS) of the University of Costa Rica and Costa Rican Institute of Electricity (ICE).

Figure 3: Distribution of dataset in terms of magnitude, distance, event type, and site class. The distribution of Douglas *et al.* (2004) and the newly added data for the period 1996-2006 are also shown for comparison.

Figure 4: Distribution of dataset in terms of magnitude, distance, focal depth, event type, and geographic region. The distribution of the Peru-Chile dataset studied in Arango *et al.* (2010) is also shown for reference.

Figure 5: Comparison of the location and depths of the Central American earthquakes used in this study, as reported in the ISC and EHB Bulletins. D_{trench} refers to the horizontal distance to the trench measured perpendicular to its local axis.

Figure 6: Map showing the locations of the subduction-zone events in Central America whose data have been used in this study. Moment magnitudes and focal mechanisms of M_W=6.0 events in the database are also indicated.

Figure 7: H/V ratios of smoothed Fourier amplitude spectra obtained at various stations of the UCA and SNET digital networks in El Salvador, using low-amplitude recordings (PGA<100 cm/s^2) from subduction events in Central America. The UDBS, SNET, ESJO, UESS stations are located on volcanic deposits. The amplification at long periods observed at CSBR is likely to be related to the extensive depth of the volcanic ash (>25 km) and at USPN, it might be the result of topographic effects. The ULLB station is located on alluvial materials underlain by lavas and HSRF station is on andesitic and basaltic materials.

Table 1: Summary of the interface and intraslab ground-motion data from the Central American subduction zone compiled in the present study, including information on record availability. A flat-file of the compiled database is available as an electronic supplement to this paper.

Country	Type	Number of events	M_W range	Depth range [km]	Number of records	R_{rup} range [km]	PGA range [cm/s^2]	Record availability[a]
El Salvador	Interface	8	5.1-5.8	24-59	88	65-399	2-66	Douglas *et al.* (2004)[b] UCA[c] SNET[d]
	Intraslab	31	5.1-7.7	54-185	313	62-295	1-1105	
Nicaragua	Interface	5	5.2-6.9	23-59	15	106-310	1-10	Douglas *et al.* (2004)[b] INETER[e]
	Intraslab	13	5.0-6.5	67-119	87	68-375	13-157	
Costa Rica	Interface	5	5.9-7.3	18-34	26	18-103	12-242	Douglas et al. (2004)[b]
	Intraslab	1	6.5	79	10	76-129	18-143	
Guatemala	Interface	4	6.3-6.9	26-64	7	46-124	10-55	Douglas *et al.* (2004)[b] CONRED[f]
	Intraslab	14	5.1-6.6	40-123	8	95-128	7-50	
All Central America	Interface	22	5.1-7.3	18-64	136	18-399	1-242	
	Intraslab	58	5.0-7.7	48-185	418	62-375	1-1105	

[a]Contact point for the various contributing agencies for record acquisition purposes. A field with the agency associated with each record is included in the flat file available as electronic supplement to this paper.
[b]Strong-motion records available on the Douglas *et al.* (2004) CD available on request from NORSAR.
[c]Interested readers shall contact Reynaldo Zelaya from the Central American University (UCA) regarding strong-motion records availability (rezelaya@ing.uca.edu.sv)
[d]Interested readers shall contact Antonio Hernandez from the National Service of Territorial Studies (SNET)) regarding strong-motion records availability (ahernandez@marn.gob.sv)
[e]Interested readers shall contact Angélica Muñoz from the Nicaraguan Institute of Territorial Studies (INETER) regarding strong-motion records availability (angelica.munoz@gf.ineter.gob.ni)
[f]Interested readers shall contact David Monterroso from the National Commission for Disaster Reduction of Guatemala (CONRED) regarding strong-motion records availability (DMonterroso@conred.org.gt)

Table 2: Information on strong-motion stations in El Salvador used in this study

Instrument and station information							Geological and geotechnical information					Site class assigned			
Name	Code	Net-work	Lat [ºN]	Lon [ºW]	IT[a]	IL[b]	Surface geology[c]	SC[d]	V_{S30}[e]	T_0[f]	$T_{0,REC}$[g]	NH[h]	NZ[i]	JP[j]	CO[k]
Acajutla, Cepa	CA	CIG	13.567	89.833	S	U	Volcanic epiclastics, pyroclastics, lava flows [1]/Intermediate intrusive rocks [2]	*B*[1]	-	-	Low amplification	B	B	I	S_1
Santiago de Maria	SM	CIG	13.486	88.471	S	S	Acid pyroclastics, volcanic epiclastics (brown tuffs)[1]	*D*[1]	-	T_1=0.19 T_2>0.60	T_1=0.19-0.24 T_2=0.85-1.00	C/D	C	III	S_3
San Miguel	MG	CIG	13.475	88.183	S	B	Acid pyroclastics, volcanic epiclastics (brown tuffs)[1]	*C*[1]	-	-	T_1=0.10-0.30	C/D	C	III	S_3
Observatorio, San Salvador	OB	CIG	13.680	89.196	S	S	Volcanic ashes (*tierra blanca*), low consolidated[1] /Acid pyroclastics, subordinate volcanic epiclastics (brown tuffs)[2]	*D*[1]	-	T_1=0.18 T_2=0.30	T_1=0.30-0.50	C/D	C	III	S_3
Sensuntepeque	SE	CIG	13.867	88.663	S	B	Volcanic epiclastics, pyroclastics, lava flows [1]	*B*[1]	-	-	Low amplification	C	B	II	S_2
Presa 15 de Septiembre	QC	CIG	13.616	88.550	S	D	Andesitic-basaltic effusives[1]	*B*[1]	-	T_1=0.27	Low amplification	C	B	II	S_2
Relaciones Exteriores [bottom of borehole - 12.5m depth]	RF	CIG	13.692	89.250	S	BB	Brown tuffs, locally with ashes and scoria[1] / Lava flows[2]	*C*[1]	-	-	Low amplification	C	B	II	S_2
Relaciones Exteriores [top of borehole]	RS	CIG	13.692	89.250	S	TB	Brown tuffs, locally with ashes and scoria[1] / Acid pyroclastics, subordinate volcanic epiclastics (brown tuffs)[2]	*D*[1]	-	T_1=0.28	Low amplification	C/D	C	II	S_2
Viveros de Dua [bottom of borehole]	VF	CIG	13.736	89.209	S	BB	Volcanic ashes (*tierra blanca*), low consolidated[1]	*C*[1]	-	-	T_1 = 0.18	C/D	C	II	S_2
Viveros de Dua [top of borehole]	VS	CIG	13.737	89.209	S	TB	Volcanic ashes (*tierra blanca*), low consolidated[1]	*D*[1]	-	T_1=0.40 T_2>0.60	T_1=0.40-0.55	D	C	III	S_3
Cutuco	CU	CIG	13.333	87.817	S	U	Andesitic- basaltic effusives [1]/Acid pyroclastics, volcanic epiclastics [2]	*B*[1]	-	-	Low amplification	B	B	I	S_1

Name	Code	Network.	Lat [ºN]	Lon [ºW]	IT[a]	IL[b]	Surface geology[c]	SC[d]	V_{S30}[e]	T_0[f]	$T_{0,REC}$[g]	NH[h]	NZ[i]	JP[j]	CO[k]
Cessa Metapan	CM	CIG	14.333	89.450	S	U	Alluvium, locally with pyroclastics[1] / Acid intermediate intrusive rocks. Tertiary[2]	*B*[1]	-	-	-	B	B	I	S_1
Santa Ana	SA	CIG	13.992	89.550	S	B	Acid pyroclastics, volcanic epiclastics (brown tuffs) [1] / Acid pyroclastics, subordi nate brown color tuffs over lava[2]	*D*[1]	-	-	T_1=0.80	D	C	III	S_3
Ciudadela Don Bosco	DB	CIG	13.733	89.150	S	U	Volcanic ashes (*tierra blanca*) - low consolidated [1]	*D*[1]	-	T_1=0.30 T_2>1.00	T_1=0.38-0.42	D	C	II	S_3
Santa Tecla	ST	CIG	13.675	89.300	S	B	Acid pyroclastics, volcanic epiclastics (brown tuffs) [1]	*D*[1]	-	-	T_1=0.20 T_2=0.60	D	C	III	S_3
Universidad Centroamericana	UC	CIG	13.679	89.236	S	B6	Brown tuffs, locally with ashes and scoria[1]	*D*[1]	246	T_1=0.30	T_1=0.30-0.40	D	C	II	S_2
Seminario San José de la Montana (Top of borehole)	SS	CIG	13.703	89.224	S	TB	Volcanic ashes (*tierra blanca*) - low consolidated [1]/Acid pyroclastics, subordinate volcanic epiclastics (brown tuffs)[2]	*D*[1]	-	-	T_1=0.50-0.60	D	C	III	S_3
Seminario San José de la Montana (Bottom of borehole)	SF	CIG	13.703	89.224	S	BB	Acid pyroclastics, subordinate volcanic epiclastics (brown tuffs)[2]	*C*[1]	-	-	T_1=0.50	C/D	B	II	S_2
Centro de Investigaciones Geotécnicas	CI	CIG	13.698	89.173	S	B2	Basaltic and andesitic lavas, predominantly from San Salvador volcano[1]	B[2]	549	T_1=0.35 T_2=0.85	T_1=0.20-0.30 T_2=0.60-0.80	C	B	II	S_2
Aeropuerto Internacional El Salvador (Terminal)	AS	CIG	13.447	89.058	S	B	Sedimentary deposits (Quaternary) [4]	-	-	-	T_1=0.60-0.80	D/E	D	IV	S_3
Instituto Geográfico Nacional, San Sal vador	IG	CIG	13.713	89.170	S	B1	Fluviatile Pumice[3] / Volcanic ashes (*tierra blanca*)[4]	C[2]	272	T_1=0.30 T_2=0.60	T_1=0.50-0.70	D	C	III	S_3
CENREN (Bottom of borehole)	CF	CIG	13.688	89.142	S	BB	Volcanic ashes (*tierra blanca*)[4]	-	-	-	T_1=0.70	D	C	III	S_3
CENREN (Top of borehole)	CS	CIG	13.688	89.142	S	TB	Volcanic ashes (*tierra blanca*)[4]	-	-	-	T_1=0.70	D	C	III	S_3
Biblioteca Nacional , San Salvador	BN	CIG	13.698	89.190	S	B	Alluvium[3]	C[2]	-	-	T_1=0.40-0.60	D	C	III	S_3
Hotel Sheraton , San Salvador	HSH	CIG	13.709	89.241	S	B8	Fluviatile pumice over lava[3]/ Volcanic ashes (*tierra blanca*)[4]	B[2]	574	-	T_1=0.22-0.24 T_2=0.80-0.90	C	B	II	S_2

Name	Code	Network.	Lat [ºN]	Lon [ºW]	IT[a]	IL[b]	Surface geology	SC[d]	V_{S30}[e]	T_0[f]	$T_{0,REC}$[g]	NH[h]	NZ[i]	JP[j]	CO[k]
Ministerio de Educacion , San Salvador	MDE	CIG	13.700	89.190	S	B4	Acid pyroclastics, subordinate volcanic epiclastics (brown tuffs)[4]	-	-	-	T_1=0.24-0.30	C/D	B	II	S_2
Instituto de Vivienda Urbana, San Salvador	MU	CIG	13.721	89.206	S	B6	Fluviatile Pumice[3] / Volcanic ashes (*tierra blanca*)[4]	B[2]	-	-	T_1=0.27 T_2=0.75	C/D	B	II	S_2
Tacuba	TAC	CIG	13.901	89.932	S	S	Acid pyroclastics, volcanic epiclastics (brown tuffs) [4]	B[2]	-	-	-	C/D	B	II	S_2
Usulutan	USU	CIG	13.344	88.438	S	S	Acid pyroclastics, subordinate volcanic epiclastics (brown tuffs)[4]	-	-	-	Low amplification	C	B	II	S_2
Aeropuerto Ilopango	AI	CIG	13.700	89.120	S	S	Volcanic ashes (*tierra blanca*)[4]	-	-	T_1=0.35 T_2>1.00	No clear peak	D/E	D	IV	S_3
Ahuachapan [Before 1996]	AHU	CIG	13.927	89.852	S	S	Acid pyroclastics, volcanic epiclastics (brown tuffs) [4]	B[2]	-	-	T_1=0.46	C/D	C	III	S_3
Ahuachapan [After 1996]	AH	CIG	13.925	89.805	S	S	Acid pyroclastics, volcanic epiclastics (brown tuffs)[1]	D[1]	-	T_1=0.6	T_1=0.55	D	C	III	S_3
Aeropuerto Internacional El Salvador	AIES	SNET	13.447	89.051	E	B	Sedimentary deposits (Quaternary)[4]	Soft soil[3]	-	T_1=0.25 T_2=0.60	T_1=0.60-0.80	D/E	C	IV	S_3
Base Naval, La Unión	LUNA	SNET	13.335	87.834	E	B	Acid pyroclastics and volcanic epiclastics [4]	Soft soil[3]	-	T_1=0.45	T_1=0.20 T_2=0.95	D/E	C	IV	S_3
Campo Experimental UCA	CEUC	SNET	13.846	89.359	SR	U	Acid pyroclastics, volcanic epiclastics (brown color tuffs)[4]	Hard soil[3]	-	T_1=0.18	Low amplification	C	B	II	S_2
Casa Presidencial (Bottom of borehole)	CPRF	SNET	13.685	89.240	SR	BB	Acid pyroclastics, volcanic epiclastics (brown color tuffs)[4]	Rock[3]	-	T_1=0.18	Low amplification	B	B	I	S_1
Casa Presidencial (Top of borehole)	CPRS	SNET	13.685	89.240	SR	TB	Acid pyroclastics, volcanic epiclastics (brown color tuffs)[4]	Hard soil[3]	-	-	Low amplification	C	C	II	S_2
Chinameca	CHIN	SNET	13.513	88.348	E	B	Acid pyroclastics, volcanic epiclastics (brown color tuffs)[4]	Soft soil[3]	-	T_1>0.60	T_1>1.0	D/E	C	IV	S_3
Ministerio de Agricultura y Ganaderia	MAGT	SNET	13.684	89.286	E	B	Acid pyroclastics, volcanic epiclastics (brown tuffs)[4]	Hard soil[3]	-	T_1=0.40 T_2>0.80	T_1=0.22 T_2>0.60	D/E	C	IV	S_3

Name	Code	Network.	Lat [ºN]	Lon [ºW]	IT[a]	IL[b]	Surface geology	SC[d]	V_{S30}[e]	T_0[f]	$T_{0,REC}$[g]	NH[h]	NZ[i]	JP[j]	CO[k]
San Jacinto	SJAC	SNET	13.674	89.198	SR	S	Acid pyroclastics, volcanic epiclastics (brown color tuffs)[4]	Soft soil[3]	-	T_1=0.18 T_2>0.80	T_1=0.55-0.70	D/E	C	IV	S_3
Acajutla	ACAJ	SNET	13.575	89.834	E	U	Volcanic epiclastics, pyroclastics, lava flows[4]	Hard soil[3]	-	T_1=0.15 T_2>0.60	Low amplification	B	B	I	S_1
San Miguel	SMIG	SNET	13.439	88.159	E	B	Sedimentary deposits (Quaternary)[4]	Hard soil[3]	-	T_1=0.16	T_1=0.25 T_2=0.80	D	C	III	S_3
Seminario San José de la Montaña (Bottom of borehole)	SEMF	SNET	13.703	89.224	SR	BB	Acid pyroclastics,subordinate volcanic epiclastics (brown tuffs)[2]	Rock[3]			T_1=0.50	C	B	II	S_2
Seminario San José de la Montaña (Top of borehole)	SEMS	SNET	13.703	89.224	SR	TB	Volcanic ashes (*tierra blanca*) - low consolidated[4] /Acid pyroclastics, subordinate volcanic epiclastics (brown tuffs)[2]	Hard soil[3]	-	-	T_1=0.50	D	C	III	S_3
Servicio Nacional de Estudios Territoriales	SNET	SNET	13.687	89.232	E	B	Tierra blanca: acid pyroclastics and subordinate volcanic epiclastics, locally acid effusives[4]	Soft soil[3]	-	-	T_1=0.42-0.46	D	C	III	S_3
Sonsonate (Agape)	SONS	SNET	13.736	89.710	E	U	Sedimentary deposits (Quaternary)[4]	Soft soil[3]	-	-	T_1=0.10-0.20 T_2>0.60	D	C	III	S_3
Unidad de Salud La Herradura	HERR	SNET	13.349	88.956	E	B	Sedimentary deposits (Quaternary)[4]	Soft soil[3]	-	-	T_1=0.20-0.25 T_2>0.70	D/E	C	IV	S_3
Unidad de Salud Perquín	PERQ	SNET	13.959	88.158	E	B	Acid pyroclastics and volcanic epiclastics[4]	Hard soil[3]	-	-	T_1=0.38-0.42	C/D	C	II	S_2
Universidad Don Bosco	UDBS	SNET	13.715	89.155	E	B	Tierra blanca: acid pyroclastics and subordinate volcanic epiclastics, locally acid effusives[4]	Soft soil[3]	-	-	T_1=0.40-0.45	D	C	III	S_3
Universidad de El Salvador	UESS	SNET	13.720	89.201	E	B	Acid pyroclastics and volcanic epiclastics[4]	Hard soil[3]	-	-	T_1=0.35-0.45	C/D	C	II	S_2
Universidad Católica de Occidente	UNCO	SNET	13.980	89.540	E	B	Acid pyroclastics, volcanic epiclastics (brown color tuffs)[4]	Hard soil[3]	-	-	T_1=0.40-0.50	C/D	C	II	S_2
Armenia	UARM	UCA	13.744	89.501	SS	B1	Acid pyroclastics, volcanic epiclastics (brown color tuffs)[1]/Soil[2]	*D*[3]	-	T_1=0.25 T_2=0.60	T_1=0.55-0.75	D/E	C	III	S_3
Externado	ESJO	UCA	13.707	89.207	SS	B1	Volcanic ashes (*tierra blanca*) - Low consolidated[1]/Soil[2]	*D*[3]	-	T_1=0.45	T_1=0.48-0.53	D	C	III	S_3

Name	Code	Network.	Lat [ºN]	Lon [ºW]	IT[a]	IL[b]	Surface geology[c]	SC[d]	V_{S30}[e]	T_0[f]	$T_{0,REC}$[g]	NH[h]	NZ[i]	JP[j]	CO[k]
Hospital San Rafael	HSRF	UCA	13.671	89.279	E	B1	Andesitic and basaltic effusives (Piroclastites)[1]/Soil[2]	*C*[1]	-	T_1=0.18	T_1=0.16-0.22	C	B	II	S_2
La Libertad	ULLB	UCA	13.486	89.327	SS	B1	Alluvium, locally with pyroclastics over lavas[1]/ Alluvium[2]	*C*[1]	-	T_1=0.18	T_1=0.16-0.20	C	C	II	S_2
Panchimalco	UPAN	UCA	13.614	89.179	SS	B1	Acid pyroclastics, volcanic epiclastics, welded tuffs[1]/Rock at the bottom of a narrow NS valley[2]	*B*[1]	2100	-	Low amplification	A	A	I	S_1
San Bartolo	CSBR	UCA	13.704	89.106	SS	B1	Acid pyroclastics (tierra blanca) [1] /Soil[2]	*D*[1]	-	T_1>0.60	T_2>0.70	D/E	D	IV	S_3
San Pedro Nonualco	USPN	UCA	13.602	88.927	SS	B1	Acid pyroclastics, volcanic epiclastics, welded tuffs[1]/Soil at crest of a EW ridge[2]	*D*[1]	-	T_1=0.40 T_2>0.80	T_1=0.40 T_2>0.80	C/D	C	III	S_3
San Vicente	HSGT	UCA	13.642	88.784	SS	B1	Acid pyroclastics (*tierra blanca*)[1]/Soil[2]	*D*[1]	-	T_1=0.18 T_2>0.80	T_2>0.60	D/E	C	III	S_3
Tonacatepeque	UTON	UCA	13.778	89.114	SS	B1	Acid pyroclastics, volcanic epiclastics, welded tuffs[1]/Soil[2]	*D*[1]	-	T_1=0.15 T_2>0.60	T_2>0.60	D	D	III	S_3
Zacatecoluca	HSTR	UCA	13.517	88.869	SS	B1	Volcanic epiclastics, pyroclastics, lava flows [1]/Soil[2]	*B*[1]	-	T_1=0.16	T_1=0.16	C/D	C	II	S_2

[a] Instrument type: E=ETNA; Q=QDR; S=SMA-1; S-R= SMA-1 Retrofitted; SS=SSA-2

[b] Instrument location: B=building, followed by number of storeys if known; S=shelter; TB=top of borehole; BB=bottom of boregole; U=unknown.

[c] Description of the surface geology based on the following references: [1] Cepeda *et al*. (2004); [2] Information listed in the accelerogram headings; [3] Douglas *et al*. (2004); [4] Geologic Map of El Salvador (SNET)

[d] Site classes assigned in previous studies. [1] NEHRP site classes assigned by Cepeda *et al*. (2004) in italics; [2] EUROCODE site dasses assigned by Douglas *et al*. (2004), underlined; [3] Site conditions assigned by Climent *et al*. (2007).

[e] Average shear-wave velocity over the top 30m, in m/s, determined by Faccioli *et al*. (1988) and listed in the Douglas *et al*. (2004) database.

[f] Predominant site period, in seconds, determined by Salazar *et al*. (2007) using surface to reference site spectral ratios and horizontal to vertical spectral ratios of earthquake records. For sites that exhibit peaks of amplification at different periods, T_1 and T_2 values are listed

[g] Site period calculated from accelerogram by considering the smoothed H/V ratio of Fourier Amplitude Spectra. The lower and upper boundaries of the interval correspond to the maximum and minimum values of the site period found when using multiple records from the same station. For sites that exhibit several peaks of amplification at different periods, T_1 and T_2 values are listed. Values are only listed for those records whose vertical component is available

[h] Site class assigned following the NEHRP (1997) provisions

[i] Site class assigned following the New Zealand site classification (McVerry *et al*., 2006)

[j] Site class assigned following the Zhao *et al*. (2006) scheme

[k] Site class assigned to compute the design loads prescribed by the 1994 El Salvador seismic code

Table 3: Information on strong-motion stations in Nicaragua used in this study

Instrument and station information							Geological and geotechnical information				Site class assigned			
Name	Code	Network.	Lat [ºN]	Lon [ºW]	IT[a]	IL[b]	Surface geology[c]	SC[d]	V_{S30}[e]	$T_{0,REC}$[f]	NH[g]	NZ[h]	JP[i]	CO[j]
Chinandega, Bayer	1662	IIS	12.610	87.120	S	U	Alluvial deposits[1]/Soft soil[3]	B[1]	-	T_1~0.25 T_2=0.60-0.80	D	C	III	Medium
Chinandega, Bomberos	1661	IIS	12.330	87.140	S	B	Alluvial deposits[1]/Soft soil[3]	D[1]	-	T_1~0.25 T_2=0.60-0.80	D	C	III	Medium
Corinto, Edificio Administrativo	COR1	IIS	12.480	87.170	S	B	Alluvial deposits[1]/Soft soil[3]	C[1]	-	T_1=0.50	D	C	III	Medium
Corinto, Muelle Norte	COR2	IIS	12.480	87.170	S	U	Alluvial deposits[1]/Soft soil[3]	D[1]	-	T_1=0.25 T_2=0.55	D	C	III	Medium
Corinto, Muelle Sur	COR3	IIS	12.480	87.170	S	U	Alluvial deposits[1]/Soft soil[3]	B[1]	-	T_1=0.15 T_2=0.45	D	C	III	Medium
Jinotepe, Palacio Municipal	1657	IIS	11.850	86.200	S	B	Volcanic rocks[1]	B[1]	-	T_1=0.20	C	B	II	Hard
Rivas, Bomberos	1665	IIS	11.430	85.850	S	B	Marine sediments[1]/Soft soil[3]	C[1]	-	T_1=0.40	C/D	C	II	Medium
Leon , Col. Calazans	1658	IIS	12.440	86.900	S	U	Alluvial deposits[1]/Soft soil[3]	D[1]	-	T_1=0.45-0.65	D	C	III	Medium
Managua, Aeropuerto Internacional	1671	IIS	12.140	86.270	S	U	Tuffs of basaltic composition and intercalated pumice and scoria[2]	C[1]	-	T_1=0.15 T_2=0.45	C/D	C	II	Medium
Managua, Aguadora	1667	IIS	12.130	86.300	S	U	Tuffs of basaltic composition and intercalated pumice and scoria[2]	D[1]	-	T_1=0.35	C	B	II	Hard
Managua, Cementera	1191	IIS	12.110	86.130	S	U	Tuffs of basaltic composition and intercalated pumice and scoria[2]	C[1]	-	T_1=0.38-0.45	C/D	C	II	Hard
Managua - Coca Cola	1669	IIS	12.110	86.250	S	U	Tuffs of basaltic composition and intercalated pumice and scoria[2]	C[1]	-	No clear peak	C	B	II	Hard
Managua - B. Amer. S2	1664	IIS	12.130	86.270	S	B17	Tuffs of basaltic composition and intercalated pumice and scoria[2] /Hard soil[3]	B[1]	-	T_1=0.40	C	B	II	Hard
Managua - Teatro Nacional	1656	IIS	12.160	86.270	S	B	Tuffs of basaltic composition and intercalated pumice and scoria[2]	C[1]	349[1]	T_1=0.42	C/D	C	II	Medium

Name	Code	Net-work	Lat [ºN]	Lon [ºW]	IT[a]	IL[b]	Surface geology[c]	SC[d]	V_{S30}[e]	$T_{0,REC}$[g]	NH[h]	NZ[i]	JP[j]	CO[k]
Managua - Instituto Sismico	1668	IIS	12.150	86.270	S	B	Tuffs of basaltic composition and intercalated pumice and scoria[2]	C[1]	-	T_1=0.15	B	B	I	Hard
Boaco	BOAN	INETER	12.473	85.658	E	U	Volcanic rock[1]	Rock[2]	-	T_1=0.15	B	B	I	Hard
Chinandega (Enitel)	CHAN	INETER	12.625	87.144	E	U	Alluvial deposits[1]	Soft soil[2]	-	T_1=0.70-0.90	D/E	D	IV	Soft
Defensa Civil, Managua	DCAN	INETER	12.124	86.267	E	B	Tuffs of basaltic composition and intercalated pumice and scoria[2]	Soft soil[2]	-	No clear peak	D	C	III	Medium
Esteli	ESAN	INETER	13.099	86.355	E	U	Volcanic deposits[1]	Soft soil[2]	-	T_1=0.60-1.0	D/E	D	IV	Soft
Granada (Enitel)	GRAN	INETER	11.937	85.976	E	U	Volcanic deposits[1]	Soft soil[2]	-	T_1=0.70	D	C	III	Medium
INETER, Managua	MGA	INETER	12.149	86.248	E	B	Tuffs of basaltic composition and intercalated pumice and scoria[2]	Soft soil[2]	-	Low amplification	C/D	C	II	Medium
Leon (Enitel)	LEAN	INETER	12.435	86.880	E	U	Alluvial deposits[1]	Soft soil[2]	-	T_1=0.15 T_2=0.80-1.0	D/E	D	IV	Soft
Masaya (Enitel)	MAAN	INETER	11.982	86.083	E	U	Tuffs of basaltic composition with intercalated pumice and scoria[2]	Soft soil[2]	-	No clear peak	D	C	III	Medium
ESSO Refineria, Managua	RAAN	INETER	12.144	86.320	E	B	Intercalated tuffs with scoria and andesitic and basaltic lavas[2]	Soft soil[2]	289[2]	T_1=0.25-0.30	D	C	II	Medium
Rivas (Enitel)	RIAN	INETER	11.439	85.829	E	U	Marine sediments[1]	Stiff soil[2]	-	T_1=0.20	C	B	II	Hard
Jinotega	JIAN	INETER	13.086	85.995	E	U	Volcanic rock[1]	Rock[2]	-	T_1=0.25	B/C	B	I	Hard

[a] Instrument type: E=ETNA; S=SMA-1

[b] Instrument location: B=building, followed by number of storeys if known; S=shelter; U=unknown.

[c] Description of the surface geology based on the following references: [1] Geologic Map of Nicaragua 1:500.000 (INETER, 1995), [2] Geologic Map of Managua 1:50.000 (INETER, 2003), [3] Segura *et al.* (1994)

[d] Site classes assigned in previous studies. [1] EUROCODE site classes assigned by Douglas *et al.* (2004), underlined; [2] Site conditions assigned by Climent *et al.* (2007).

[e] Average shear-wave velocity over the top 30m, in m/s, determined from profiles obtained by: [1] Parrales and Picado (2001); [2] Faccioli *et al.* (1973).

[f] Site period calculated from accelerogram by considering the smoothed H/V ratio of Fourier Amplitude Spectra. The lower and upper boundaries of the interval correspond to the maximum and minimum values of the site period found when using multiple records from the same station. For sites that exhibit several peaks of amplification at different periods, T_1 and T_2 values are listed. Values are only listed for those records whose vertical component is available

[g] Site class assigned following the NEHRP (1997) provisions

[h] Site class assigned following the New Zealand site classification(McVerry *et al.*, 2006)

[i] Site class assigned following the Zhao *et al.* (2006) scheme

[j] Site class assigned to compute the design loads prescribed by the 1983 Nicaragua seismic code

Table 4: Information on strong-motion stations in Costa Rica used in this study

Instrument and station information							Geological and geotechnical information				Site class assigned			
Name	Code	Net-work	Lat [ºN]	Lon [ºW]	IT[a]	IL[b]	Surface geology[c]	SC[d]	T_0[e]	$T_{0,REC}$[f]	NH[g]	NZ[h]	JP[i]	CO[j]
Alajuela	ALJ	LIS	10.021	-84.216	S	B2	Quaternary volcanic deposits (Soft soil) [1]	B	T_1=0.40	T_1=0.70	D	C	III	S_3
Boruca	APBO	LIS	8.950	-83.330	S	S	Tertiary sedimentary rocks: (massive limestone) [3]/Rock[4]	A	-	Low amplification	B	B	I	S_1
Cachi	CCH	LIS	9.843	-83.806	S	D	Tertiary volcanic materials (Rock) [1]/Rock[4]	-	-	Low amplification	B	B	I	S_1
Cartago	CTG	LIS	9.867	-83.892	S	S	Recent alluvial sediments (Soft soil) [1]	B	-	T_1=0.40 T_2=0.70	D	C	III	S_3
Geotermico	APGM	LIS	10.700	-85.190	S	S	Stiff soil[3]	C	-	T_1=0.20	C	B	II	S_2
Golfito	GLF	LIS	8.645	-83.172	S	B2	Cretaceous igneous and sedimentary materials (Soft soil) [1]/Cretaceous volcanic deposits (Rock) [2]	A	T_1=0.33	T_1= 0.30-0.37	C	B	II	S_1
Puriscal	PCL	LIS	9.845	-84.310	Q	B2	Tertiary volcanic materials (Soft soil) [1]	-	-	T_1= 0.40-0.50	D	C	III	S_3
Quepos	QPS	LIS	9.431	-84.166	S	B1	Rock and Tertiary sediments[1]/Rock[4]	A	-	Low amplification	B	B	I	S_1
San Isidro	ISD	LIS	9.373	-83.705	S	B2	Tertiary Sediments (Hard soil)[1]/Soft soil[4]	B	T_1=0.45	T_1=0.40	C	B	II	S_2
Sandillal	APSD	LIS	10.460	-85.100	S	B	Quaternary volcanic rocks. Pumiceous tuff [3]/Hard soil[4]	B	-	Low amplification	B	B	I	S_1
Savegre	APSA	LIS	9.470	-83.990	S	B	Tertiary Sedimentary Rocks. Sandstone[3]	B	-	Low amplification	B	B	I	S_1
San Ramon	SRM	LIS	10.087	84.485	S	B1	Quaternary sediments (Soft soil)[1] /Soft soil[4]	B	-	T_1=1.05	D/E	D	IV	S_4
Puntarenas - Hospital M. Sanabria	PTS	LIS	9.976	-84.751	S	B20	Quaternary coastal sediments (Soft soil) [2]/Very soft soil[4]	C	-	T_1= 0.90	D/E	D	IV	S_4
Siquirres	APQS	LIS	10.040	-83.500	S	S	Rock[3]/Colluviums and lavas[5]	A	-	T_1=0.35	B	B	II	S_1

Name	Code	Net.	Lat [ºN]	Lon [ºW]	IT[a]	IL[b]	Surface geology[c]	SC[d]	T_0[e]	$T_{0,REC}$[f]	NH[g]	NZ[h]	JP[i]	CO[j]
Sangregado	APSG	LIS	10.480	-84.760	S	B	Soft soil[3]/Hard soil[4]	C	-	T_1=0.50	D	C	III	S_3
San Jose - Guatuso	GTS	LIS	9.870	-84.038	S	B1	Tertiary sedimentary materials[1]/Soft soil[4]	-	-	T_1= 0.60	D	C	III	S_3
San Jose - Banco Nacional	BNC	LIS	9.937	-84.083	S	B20	Quaternary volcanic deposits (Stiff soil)[1]/Soft soil[4]	-	-	T_1=0.60	D	C	III	S_3
San Jose - Escuela Catolica Activa	ECA	LIS	9.936	-84.097	S	B	Volcanic deposits (Stiff soil)[3]/Soft soil[4]	B	T_1=0.25 T_2=0.50	T_1=0.50	C/D	C	III	S_3
San Jose - Hatillo	HTO	LIS	9.916	-84.099	S	B1	Recent alluvial sediments (Soft soil)[2] / Soft soil[4]	-	-	T_1=0.15 T_2=0.35	C/D	C	II	S_2
San Jose - Hotel Aurola	AUR	LIS	9.938	-84.078	S	B17	Quaternary volcanic deposits (Stiff soil)[1]/Soft soil[4]	-	-	Low amplification	C/D	C	II	S_2
San Jose - La Lucha	ALCR	LIS	9.740	-84.010	S	S	Rock[3]/Intrusive diorite [5]	A	-	Low amplification	B	B	I	S_1
San Jose - Universidad de Costa Rica (Biblioteca)	CMA	LIS	9.937	-84.054	S	B4	Quaternary volcanic deposits (Soft soil)[1]	-	T_1=0.29	T_1=0.40	C/D	C	II	S_2

[a] Instrument type: Q=QDR; S=SMA-1

[b] Instrument location: B=building, followed by number of storeys if known; S=shelter; D=Dam.

[c] Description of the surface geology based on the following references: [1] EERI (1991); [2] Taylor *et al.* (1994); [3] Douglas *et al.* (2004); [4] Climent *et al.* (2007); [5] Climent *et al.* (1992)

[d] EUROCODE site classes assigned by Douglas *et al.* (2004), underlined.

[e] Predominant site period, in seconds, determined by Moya *et al.* (2000) using the spectral ratio technique. For sites that exhibit peaks of amplification at different periods, T_1 and T_2 values are listed

[f] Site period calculated from accelerogram by considering the smoothed H/V ratio of Fourier Amplitude Spectra. The lower and upper boundaries of the interval correspond to the maximum and minimum values of the site period found when using multiple records from the same station. For sites that exhibit several peaks of amplification at different periods, T_1 and T_2 values are listed. Values are only listed for those records whose vertical component is available

[g] Site class assigned following the NEHRP (1997) provisions

[h] Site class assigned following the New Zealand site classification (McVerry *et al.*, 2006)

[i] Site class assigned following the Zhao *et al.* (2006) scheme

[j] Site class assigned to compute the design loads prescribed by the 2002 Costa Rica seismic code

Table 5: Information on strong-motion stations in Guatemala used in this study

Instrument and station information							Geological and geotechnical information			Site class assigned			
Name	Code	Network	Lat [ºN]	Lon [ºW]	IT[a]	IL[b]	Surface geology[c]	SC[d]	$T_{0,REC}$[e]	NH[f]	NZ[g]	JP[h]	CO[i]
Nuevo Hospital Militar	HMG	CONRED	14.629	-90.473	Q	B	Pumice (Quaternary)	Hard soil	T_1=0.60-0.80	D	C	III	S_2
Planta de agua Lo de Coy	PLCG	CONRED	14.621	-90.601	Q	U	Pumice (Quaternary)	Hard soil	T_1=0.20 T_2=0.95	D	C	III	S_2
Planta de agua El Cambray	PECG	CONRED	14.573	-90.489	Q	U	Pumice (Quaternary)	Hard soil	No clear peak	C	B	II	S_1
IGSS de Pamplona	IGSS	CONRED	14.606	-90.533	Q	U	Pumice (Quaternary)	Hard soil	No clear peak	C	B	I	S_1
Hospital de Salud Mental	HSMG	CONRED	14.664	-90.478	Q	B	Pumice (Quaternary)	Hard soil	T_1=0.22 T_2>1.0	D	C	III	S_2
Escuela Rosa Pardo de Lanuza	ERPG	CONRED	14.631	-90.485	Q	B	Alluvial deposits (Quaternary)	Soft soil	T_1=0.16-0.22 T_2>0.6	D/E	C	IV	S_3
Municipalidad de Villa Canales	MVCG	CONRED	14.482	-90.533	Q	U	Alluvial deposits (Quaternary)	Hard soil	No clear peak	C/D	C	II	S_2
Municipalidad de Palín	MPG	CONRED	14.403	-90.670	Q	U	Lahars and Quaternary alluvial deposits	Soft soil	T_1=0.25 T_2=0.80	D/E	C	III	S_3
Gobernación de Escuintla	GEG	CONRED	14.299	-90.785	Q	B	Lahars and Quaternary alluvial deposits	Soft soil	T_1=0.50	D	C	III	S_2
Empresa Portuaria Quetzal	EPQG	CONRED	13.939	-90.782	Q	B	Alluvial deposits (Quaternary) [1]	Soft soil	T_1=0.50	D/E	C	III	S_3

[a] Instrument type: Q=QDR

[b] Instrument location: B=building, followed by number of storeys if known; S=shelter; U=unknown.

[c] Description of the surface geology based on the 1:250.000 Geologic Map of Guatemala (IGN, 1993).

[d] Site classes assigned by Climent *et al*. (2007).

[e] Site period calculated from accelerogram by considering the smoothed H/V ratio of Fourier Amplitude Spectra. The lower and upper boundaries of the interval correspond to the maximum and minimum values of the site period found when using multiple records from the same station. For sites that exhibit several peaks of amplification at different periods, T_1 and T_2 values are listed. Values are only listed for those records whose vertical component is available

[f] Site class assigned following the NEHRP (1997) provisions

[g] Site class assigned following the New Zealand site classification (McVerry *et al.*, 2006)

[h] Site class assigned following the Zhao *et al.* (2006) scheme

[i] Site class assigned to compute the design loads prescribed by the 1996 Guatemala seismic code

Figure 1

Click here to download colour figure: JOSE455_CA_REV1_Fig1.eps

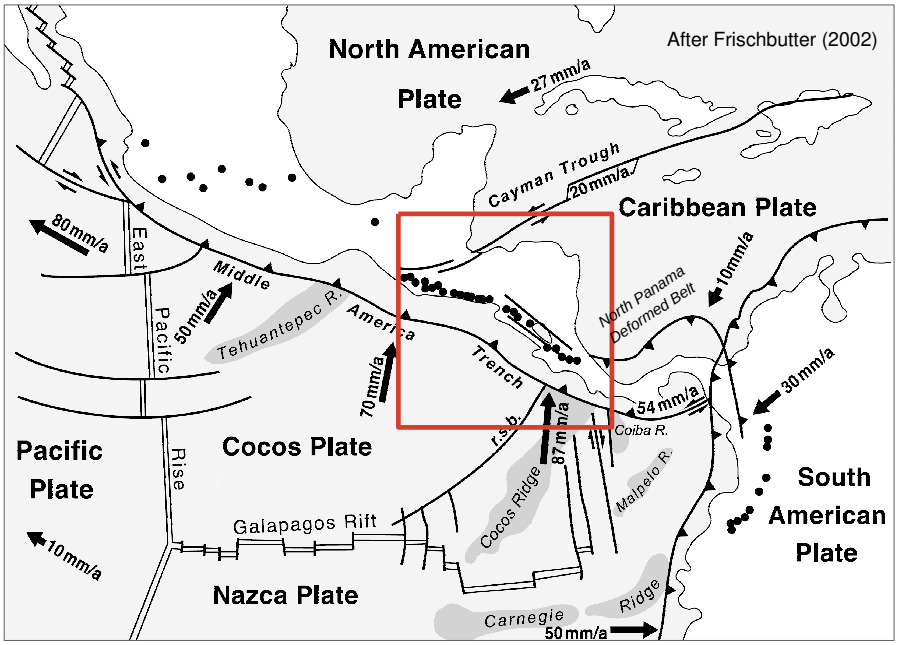

Seismicity 1960 - 2006 (EHB Catalogue)

- 0 < h ≤ 50 km
- 50 < h ≤ 100 km
- 100 < h ≤ 150 km
- 150 < h ≤ 200 km
- 200 < h ≤ 250 km
- 250 < h ≤ 300 km
- h > 300 km
- Middle American Trench
- Syracuse *et al.* (2008) Tomography profiles
- Events used in this study

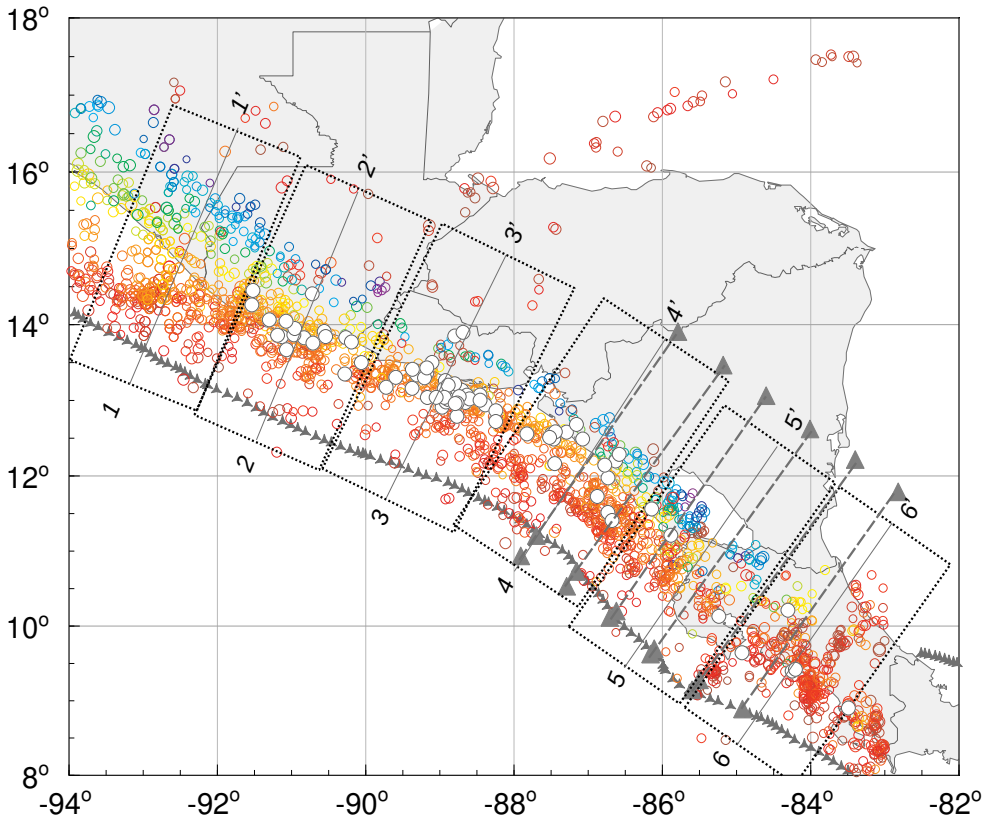

Section 1-1' [Mexico-Guatemala]

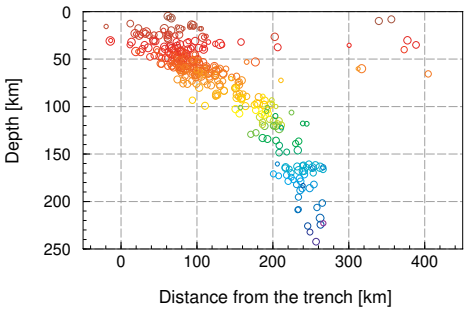

Section 2-2' [Guatemala]

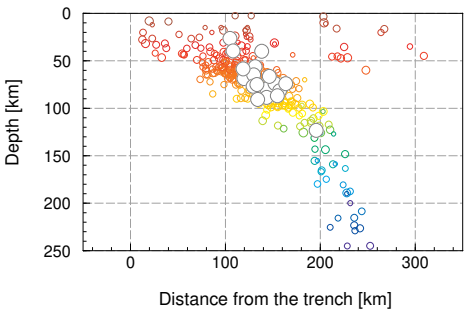

Section 3-3' [El Salvador]

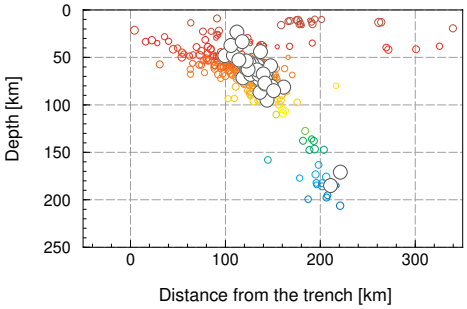

Section 6-6' [Costa Rica]

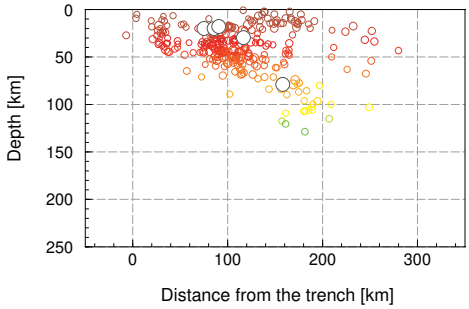

Section 5-5' [Nicaragua-Costa Rica]

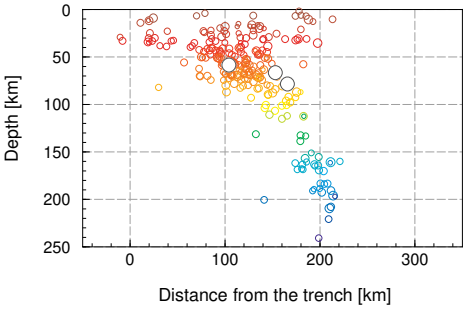

Section 4-4' [Nicaragua]

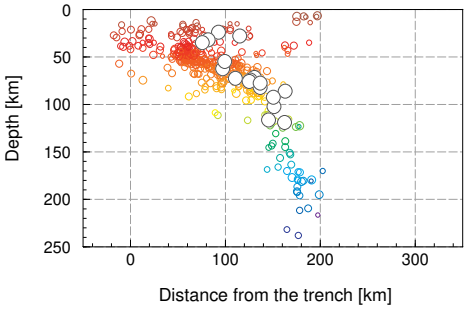

Figure 2

Click here to download colour figure: JOSE455_CA_REV1_Fig2.eps

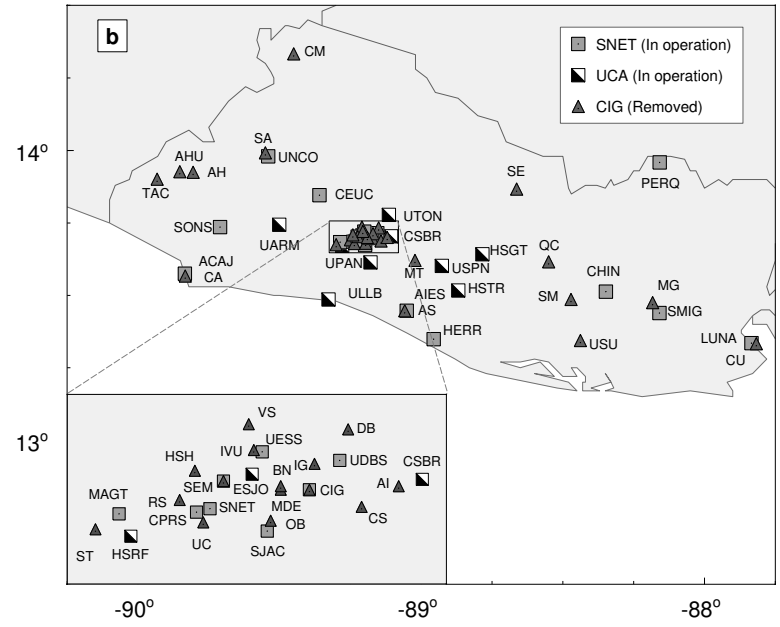

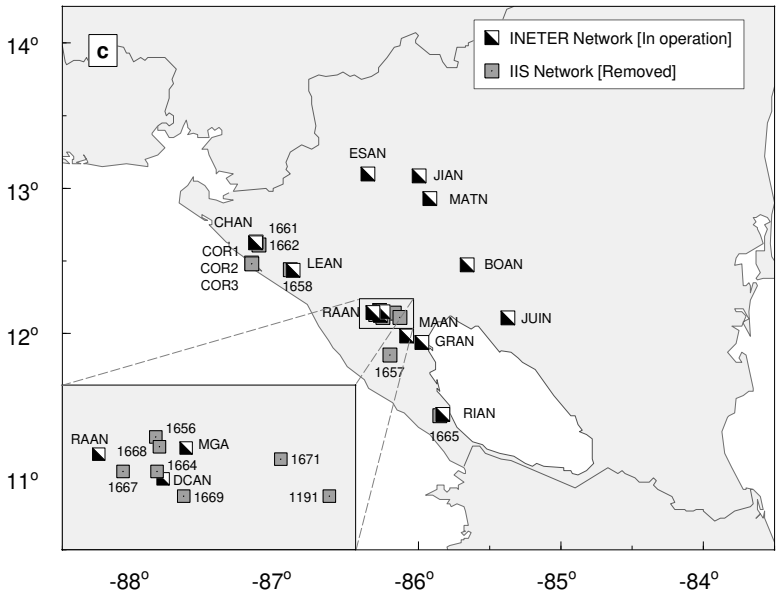

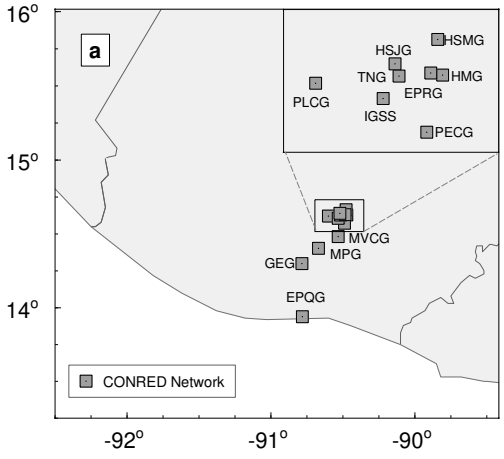

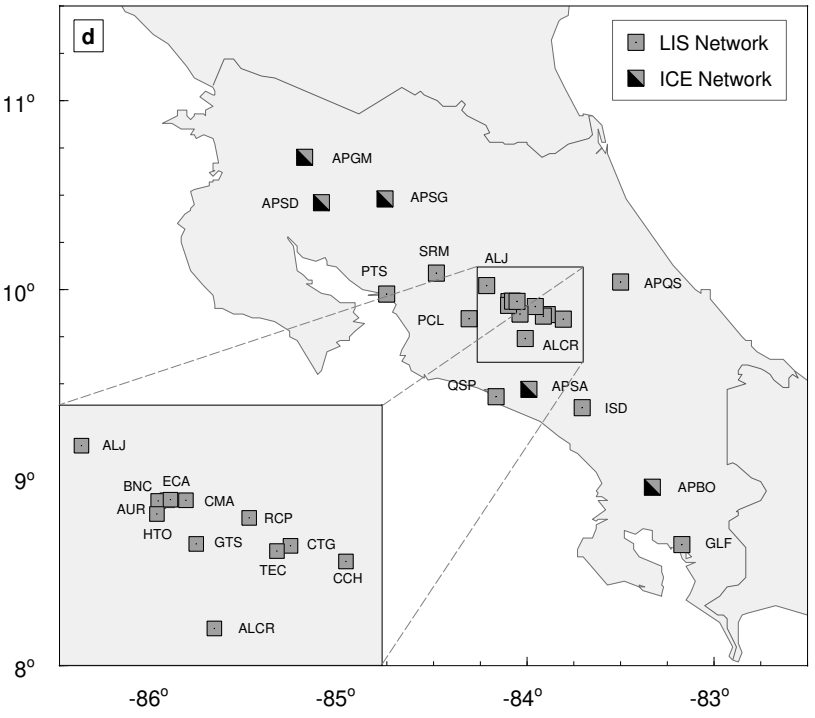

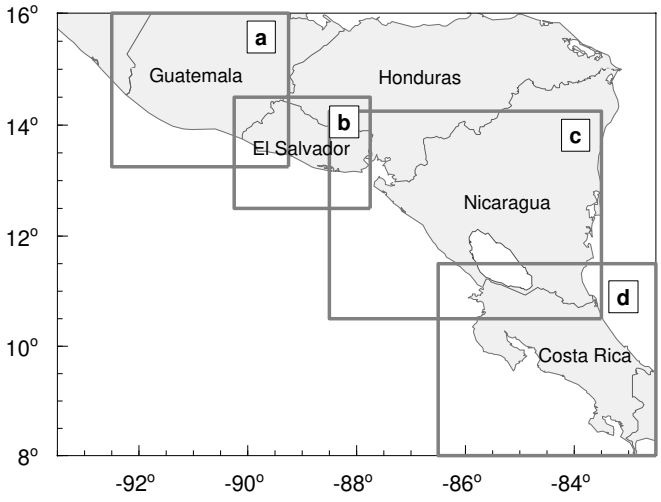

Figure 3

Click here to download colour figure: JOSE455_CA_REV1_Fig3.eps

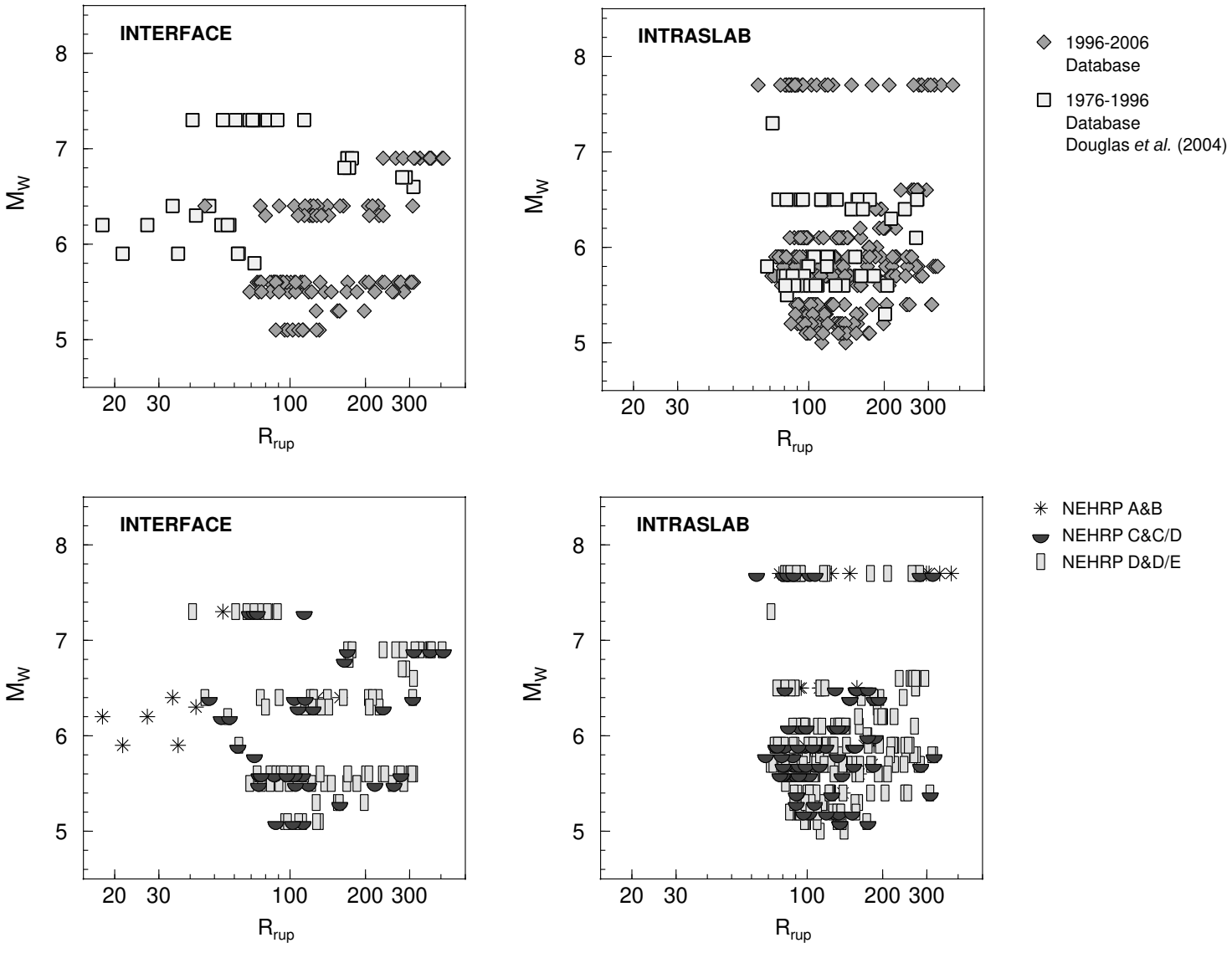

Figure 4

Click here to download colour figure: JOSE455_CA_REV1_Fig4.eps

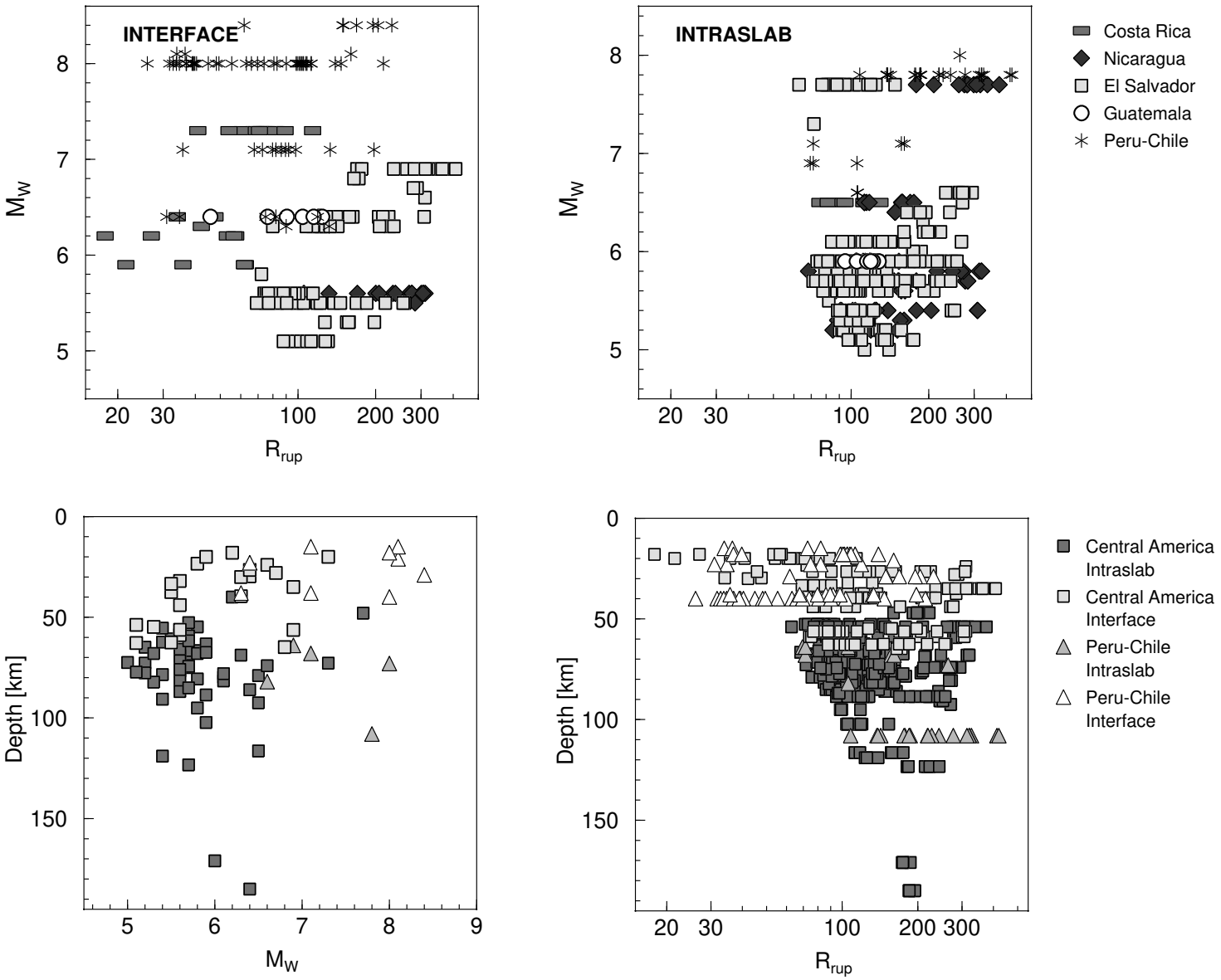

Figure 5
Click here to download colour figure: JOSE455_CA_REV1_Fig5.eps

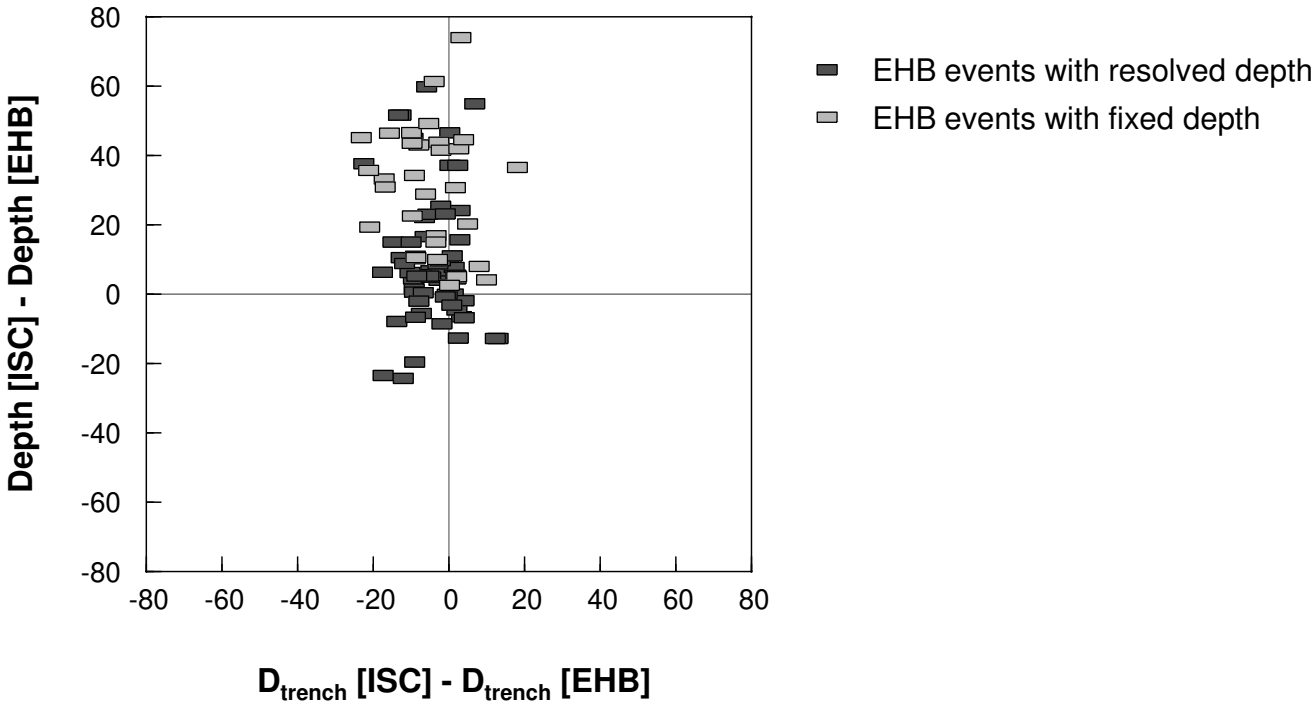

Figure 6

Click here to download colour figure: JOSE455_CA_REV1_Fig6.eps

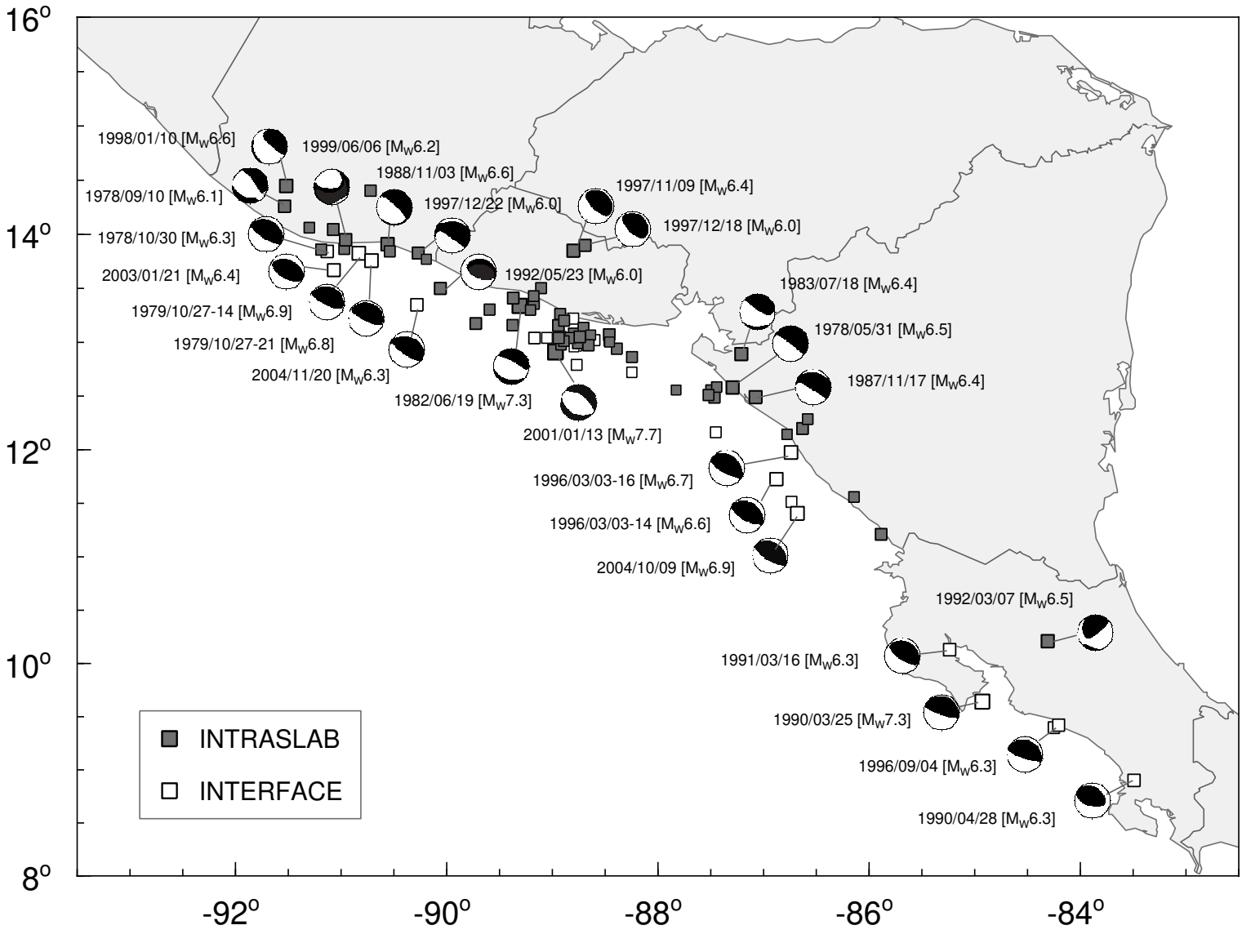

Figure 7

Click here to download colour figure: JOSE455_CA_REV1_Fig7.eps